Earthquake Relocation in the Northeastern Side of MMT and Its Implication on the Seismogenic Structure

BY

Humaira Bashir

Department of Earth Sciences

QUAID-I-AZAM UNIVERSITY

Islamabad-Pakistan

2023

Earthquake Relocation in the Northeastern Side of MMT and Its Implication on the Seismogenic Structure

BY

Humaira Bashir

A Thesis Submitted in

Partial Fulfillment of the Requirements of the

Degree Of Masters of Philosophy

in

Geophysics

Department of Earth Sciences

QUAID-I-AZAM UNIVERSITY

Islamabad-Pakistan

2023

Earthquake Relocation in the Northeastern Side of MMT and Its Implication on the Seismogenic Structure

BY

Humaira Bashir

Approved by

_____

(Associate Prof. Dr. Mumtaz Muhammad Shah)

(HOD, Department of Earth Science)

Approved by

_____

(Associate Prof. Dr. Shazia Naseem)

(Supervisor)

_____

(External Examiner)

Dedicated to My Dear Parents

LIST OF CONTENT

LIST OF ABBREVIATIONS

HypoDD	Hypocentral Double-Difference
MMT	Main Mantle Thrust
HKSZ	Hazra Kashmir Seismic Zone
IKSZ	Indus Kohistan Seismic Zone
JHD	Joint Hypocenter Determination
MSMS	Network of Micro Seismic Monitoring System
MBT	Main Boundary Thrust
IKLA	Indus Kohistan Ladak Arc
PTS	Punjal Thrust Structure
HKS	Hazara Kashmir Syntaxis
FMS	Focal Mechanism Solution
NW	North West
SE	South east
EGM	Earth gravitational model

TABLE OF CONTENT

LIST OF FIGURES

LIST OF TABLES

ACKNOWLEDGEMENT

In the name of Allah Almighty, the Most Merciful and the Most Beneficent. Journey is more important than the destination. As this journey in my life has come to an end, I wish to express my heartiest appreciation to those who have helped me in the pursuit of my MPhil degree. First of all, I am thankful to Allah Almighty. He always bestowed me far better than what I deserved. I would like to express my deepest regard to my supervisor Dr. Shazia Naseem and co-supervisor Dr. Shahid Riaz for their patience, guidance, support, and insight that they extended in my research work. Their kindness, encouragement, and faith in me throughout have been tremendously helpful for me to become a better researcher.

I am thankful to have opportunity to study in Department of Earth Sciences, QAU. I have been fortunate to have worked with professionals who have rejoiced with me in my success and supported me when I need it.

No acknowledgement would ever adequately express my feelings to my adorable family without whom I felt myself incomplete. Words become meaningless when I have to say thanks to my parents, who have been always a source of support, encouragement, and inspiration to me. Without them, I could not be able to succeed and reach at this point in life. I would also like to express my heartiest gratitude for my other family members.

Everlasting thanks to my friends for their moral support, encouragement and valuable suggestions regarding my research. I need to express my gratitude and deep appreciation to my friends whose friendship and hospitality has supported me during this time.

Today, I pray to Allah to give me the enthusiasm to serve humanity towards the right path.

Humaira Bahir

Abstract

The present study aimed to relocate earthquakes and identify seismogenic structure in the eastern side of Main Mantle Thrust in the NW Himalayas, Pakistan, based on double difference earthquake relocation, HypoDD, algorithm. The current study used 15561 earthquakes recorded over 25 stations from year 2010 to 2021 were acquired from Micro Seismic Monitoring System (MSMS) WAPDA. In total, 130043 P phases and 56107 S phases are used to relocate the earthquakes. The HypoDD algorithm relocates 6426 earthquakes. The results of relocated seismicity, Free Air Gravity Model (EGM2008), and Focal Mechanism Solutions (FMS) are used to deduce the seismogenic structure of the region. The study's results showed that the HypoDD method significantly reduced the travel time residual 66 ms compared to the initial travel time 154 ms. After earthquake relocations, it is observed that mostly earthquakes are clustered at an average depth of 5 to 30 km and a few earthquakes are observed around depth of 50 km. Additionally, the seismicity distribution pattern shows low dip angle and NE trend which was consistent with focal mechanism solutions that indicates the presence of thrust faults with minor component of strike slip in the vicinity of MMT. The northeast-trending faults were inferred from the present study, specifically, in the Indus Kohistan Seismic Zone (IKSZ) which is considered as tectonically most active region. Furthermore, finding also showed a positive association among sharp gradient in free air gravity and dense seismicity. Thus, the current study can aid in hazard analysis, improving velocity models and tomographic studies.

Chapter 1

Introduction

1.1 Overview

Major tectonic features such as syntaxis in western Himalayas were formed as a result of the collision of India and Asia and the subduction that followed the complex tectonic structure has caused shallow to deep seismicity during the past two decades, and determining the precise location of the hypocenter is a significant challenge for seismic hazard assessments (Rahman et al., 2022). The purpose of the current study is to analyze the seismogenic environment of the eastern side of the main mantle thrust. It is based on earthquake hypocentral relocation utilizing the Double-Difference Earthquake Relocation Method (HypoDD) (Waldhauser & Elseworth, 2000). Northeastern MMT the study region is located between latitudes 34^0N and 35.5^0N and longitudes 71.5^0E to 74^0E.The tectonic border between the Indian and Eurasian plates within a 250 km radius, which includes the MMT, MBT, and HKS thurst systems with splys, are the major seismic source activity, specifically the Indus Kohistan Seismic Zone (IKSZ). and the Hazra Kashmir Seismic Zone (HKSZ).

When doing a seismic hazard analysis to determine the earthquake origin zone, precise earthquake hypocenter positions are essential. As a result, the seismic source must contain the hypocenter of the earthquake recorded in the database (catalogue). For the sake of calculating the earthquake risk, there were multiple instances where the earthquake position was off from its origin place. Estimation of earthquake hypocenters has proven to be very challenging.

Around the world, a number of approaches have been tested and put to use on a variety of data sets. Iterative and completely non-linear relocation (SED) (Spence, 1980), Joint

Hypocenter Determination (JHD) (Pujol. 2000; Kim et al., 2005), and HypoDD are three or more established methods for relocating earthquakes that have been used in recent decades. Geiger's method or Single Earthquakes Determination is one of these methods. The Geiger approach (technique) seeks the smallest discrepancy between the theoretical and observed arrival times through iterative least-squares optimization (Maneno, 2019). The JHD technique, developed by Douglas (1967) , improved earthquake localization accuracy based on seismic station calibration. P- and S-wave differential travel-time observations between seismic stations from adjacent earthquakes are calculated using the Double Difference (HypoDD) method (Waldhauser & Ellsworth, 2000). The earthquake position might be successfully relocated using this method to find its associated origin. The current research provide earthquake relocation using the HypoDD for earthquake occurrences between 2010 and 2021.

The core idea of the HypoDD is first described in the following chapters, followed by sections on the geology and seismo-tectonics of the research region. The study's justification and goals for the research are then discussed. After that, seismic data from the WAPDA Network of Micro Seismic Monitoring System (MSMS) database is used to apply the technique. Then, it is compared with the pre-relocated (actual data) and relocated (processed) earthquake data. In the end, residual analysis is used to verify the reliability of the relocated hypocenter results which are discussed later in connection with FMS and association with gravity anomalies (Figure 1.1).

1.2 Study Area

In the NW Himalayas of northern Pakistan, a zone with a high level of tectonic activity, our study area is situated at 34^0N to 35.5^0N latitude and 71.5^0E to 74^0E longitude. This region is geologically and tectonically complex due to active convergence and transpression, which are defined on a regional scale. The Main Boundary Thrust (MBT), Punjal Thrust Structure (PTS),

Indus Kohistan Ladak Arc (IKLA), and Hazara Kashmir Syntaxis (HKS) are among the region's most active fault systems and are known to cause destructive earthquakes and categorized the study area is made up of the Indus Kohistan Seismic Zone (IKSZ) and the Hazara Kashmir Seismic Zone (HKSZ) based on seismic data (Khwaja et al., 2005). There are formations called Hazara, Salkhala, Kingriali, and Tanawul in the area around the Tarbela dam, which is situated in one of the NW Himalayas' most seismically active places in the lower Himalayas. According to Johnson (2002) receiver function studies by Li and Mashele (2009), the Moho significantly deepens (52–76 km) from the lower to the Himalayas.

1.3 Data and Method

1.Earthquake Data

In order to perform the analysis of relocation, this study employed a dataset of about 15561 earthquake occurrences from 2010 to 2021 provided by the WAPDA Tarbela Dam Project's micro-seismic monitoring system (MSMS) in Northern Pakistan. The HypoDD approach was used to relocate the earthquake.

2.Free Air Gravity Data (EGM2008)

Free air gravity is thought to represent variations in subsoil density. Accurate global and very high resolution data of the Earth's gravitational potential are essential for numerous geodetic, geophysical, and oceanic studies and applications (Engen et al., 2003). Additionally, it has the fewest assumptions and surveys are carried out at a constant altitude, making it the anomaly type that is most frequently utilized in research (Factor, Kenyon, Holmes, & Pavlis, 2008).

3.Focal Mechanisms Solutions

Research purposes, the focal mechanism solutions from 01-01-1976 to 24-1-2021 were obtained from (https://www.globalcmt.org/CMTsearch.html). Focal mechanisms are geometrical or mathematical representations of the faulting that takes place during an earthquake. The latter, to put it simply, is made up of the relative motions of two crustal earth blocks known as walls along a fault line. The rake or slip angle indicates the movement of the hanging wall with regard to the foot wall both inside the fault plane and with respect to the horizontal. The fault's trajectory is shown by the strike angle (relative to North) on a horizontal plane that resembles the Earth's surface. For a thorough description of the earthquake and, consequently, for the size or magnitude of the earthquakes, an additional scalar related to the length of slip of the fault walls is required (Stein, & Okal, 2005). The type of slip experienced during an earthquake, such as strike-slip, normal slip, thrust (reverse), or any combinations of these, is graphically represented by a focal mechanism, often known as a "beachball." Additionally, it shows which direction the slipping fault was. The origion of an earthquake is known as the hypocenter, and the 2-dimensional focal mechanism circle that surrounds it is actually the fault orientation projected onto the bottom half of a sphere.

1.4 Rationale of Study

Precise relative hypocenter locations and earthquake focal mechanisms are necessary to comprehend the subsurface structures (tectonic framework) of a seismically active area. Hypocenter clusters are the only readily available data set for identifying the orientations of potential seismogenic faults in the seismic zone. Relocating earthquake hypocenters in the Indus Kohistan Seismic Zone (IKSZ) of the NW Himalayas is the main objective of the current study as a consequence (Shah et al., 2022). The current study also attempts to relocate earthquakes

utilizing HypoDD, as this approach is rarely used in other studies to achieve the aforementioned goal.

Additionally, focal mechanisms substantially facilitate the interpretation of the relocation effort's results (HypoDD). This work combines several techniques; HypoDD, Gravity, and FMS to precisely identify seismogenic structure and to improve the results' external validity. These findings can be utilized to reduce seismic risk factors and to take the necessary precautions to avoid destruction and damage. In order to create a trustworthy high-resolution tomographic model, the current work is based on a scale dataset of the 2010 to 2021 recorded from neighborhood seismic stations. To precisely localize the earthquake and predict future earthquakes in that region, only local data sets were chosen. Regional data are useful as well, but local information allows researchers to determine the near source location of seismogenic structures. The pre-earthquake actions are simple to comprehend, illustrate, and put into practice in the proper location. As eastern side of MMT in the northwest Himalayas region is particularly seismically active, it may be a cost-effective and practical way to deal with natural risks.

1.5. Objectives of the Study

1. The current study intended to compute earthquake hypocenter relocation using difference in travel times by HypoDD method.
2. The study aims to understand the seismogenic environment of seismically active region and mechanism of structural evolution of Northeastern side of MMT, Pakistan.
3. To understand faults geometry in the study region. Furthermore, it also aims to explore relationship between seismicity and gravity variations.

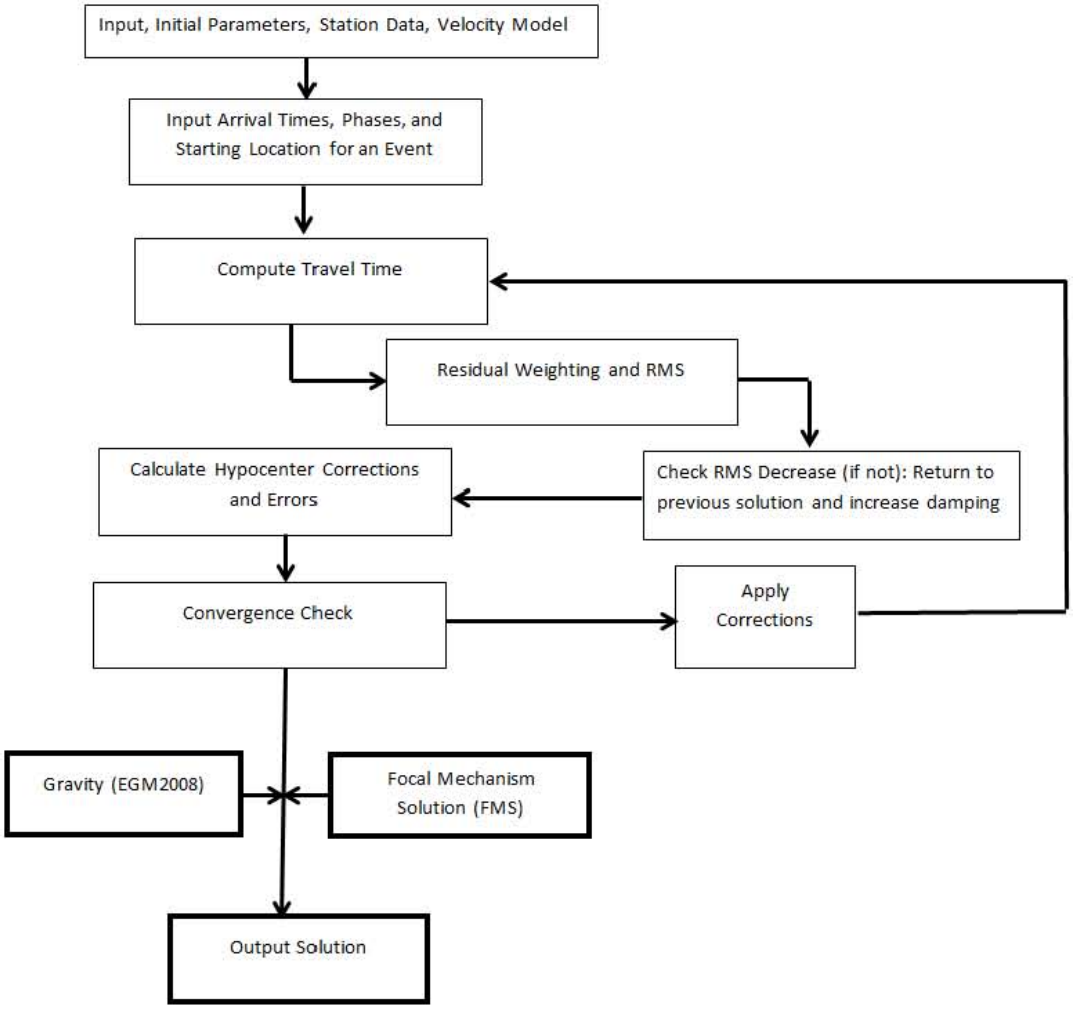

Figure 1.1: Conceptual framework of the study

Chapter 2
Seismo-Tectonics of Study Area

2.1 Overview

The Himalayas, world's newest and highest mountain, which were created because of Indian-Asian collision and Indian subduction (Li et al., 2008). According to Martin (2017) based on various crustal scale faults northwest Himalayas further divided into Lesser Himalaya, Sub-Himalaya and Higher Himalaya. Active convergence and transgression both are defined by this region's complex geology and tectonics. Major active fault systems on a regional scale include the Punjal Thrust Structure (PTS), Indus Kohistan Ladak Arc (IKLA), and Hazara Kashmir Syntaxis (HKS), making this area more susceptible to devastating earthquakes (MonaLisa et al., 2008). According to them the seismic zones of IKSZ and HKSZ are distinguished by seismic zonation of Pakistan, based on the previous seismic records. The area surrounding in the Tarbela Dam MSMS network, which is monitoring seismic activity in Himalayas characterized one of the most seismically active areas is the vicinity of MMT in NW Himalayas. According to previous study (Shah et al., 2022). The Indus Kohistan seismic zone, Hazara Kashmir syntaxes zone, the Peshawar Hazara seismic zone, and the MBT seismic zone are more earthquake hazard prone, as guided by the PGA map and resulting hazard spectra.

In addition to, the study area has elevation range from 2000 m to 5000 m and consists of ridges and valleys topographic features .Moreover, it contains the formations Hazara, Salkhala, Kingriali, and Tanawul.

Keeping its tectonically complex structure and high seismicity in mind, the current study select the 71.5^0E to 74^0E longitude and 34^0N to 35.5^0N latitude ranges in in the eastern side of Main Mantle Thrust in northwestern Himalayas, Pakistan.

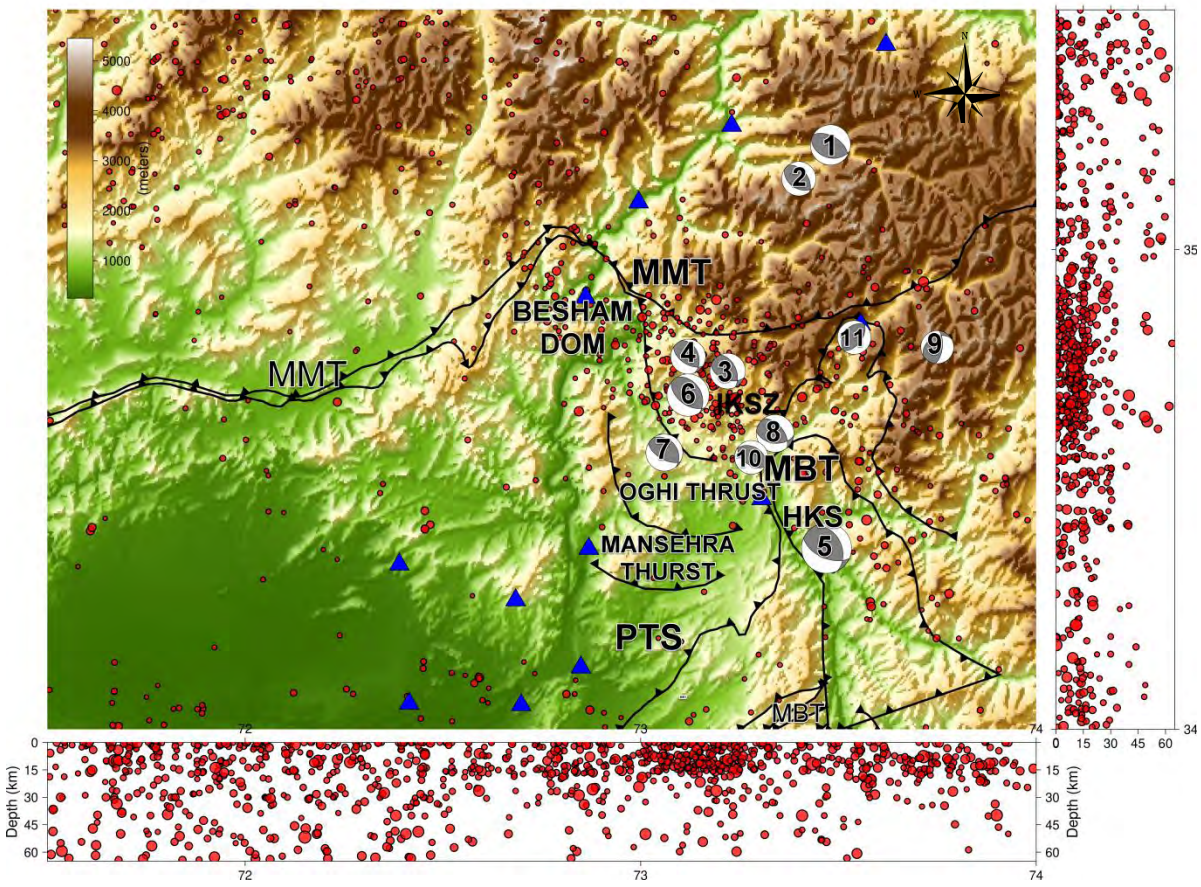

Figure 2.1: Study area map with topography and seismo-tectonics and stations (blue triangles) distribution. The earthquakes (red circle) location estimated by WAPDA MSMS and FMS derived from www.gcmt.org, while IKSZ,HKS,MMT,MBT and PTS are major seismogenic stuctures in the study area.

2.2 Geology and Seismo-Tectonics of the Study Area

Understanding a seismically active area's underlying features (tectonic framework) need exact relative hypocenter positions (locations) and earthquake focal mechanisms. Hypocenter clusters are the sole data set available for assessing the orientations of likely seismogenic faults in the seismic zone. As a result, the present study's major purpose is to relocate earthquake hypocenters in the MMT specifically Indus Kohistan Seismic Zone (IKSZ) of the NW Himalayas. Previous researchers Li et al. (2008) and Zhao et al. (2016) indicates that the geometry of the under thrusts in the Central and Eastern Himalayas and Indian and Eurasian plates in the Western Himalayas is significantly (greatly) different. The region's most notable

tectonic structures are the Main Mantle Thurst (MMT), Nanga Parbat Syntaxis (NP), Main Boundary Thurst (MBT) and the Hazra Kashmir Syntax (HKS). Another study revealed that the Indian plate's northward migration switched translation to translation-cum-rotation, causing the structural alignment of the NP and HKS to be at a right angle to each other (Sana & Nath, 2016).

In the northwest Himalayas, the IKSZ is a northwest striking zone. IKSZ follows the Hazara Kashmir Syntaxis (HKS) along the Main Boundary Thrust (MBT), which is located about 50 kilometres from Tarbela dam and characterized by thrust earthquakes with depths ranging from 30 to 40 kilometres. The Indus Kohistan-Ladakh Arc formed during the Jurassic-Cretaceous period as a result of a northward dipping subduction zone in the Tethys Ocean's equatorial region (Torii & Zaman 1999; Yoshida et al., 1996). The study cuducted by Shah et al. (2022) demonstrated that the Kohistan Arc (KLA) originally collided with the Asian plate in the north during the Early Cretaceous, then collided with and over thrusted the Indian plate in the south during the Mid-Eocene.

Earthquakes along the IKSZ there in NW Himalayas are mainly shallow depths and have reversal processes with NE to SW compression (Wallace & Fan, 1994). The FMS along the IKSZ point to the Indian plate subducting northeast under the KLA (Das & Pegler, 1998). In addition, Tahirkheli (2010) revealed that the strong crustal seismicity may have resulted from the close contact of the northern end of the Hazara Kashmir Syntaxis with the western half of MMT.

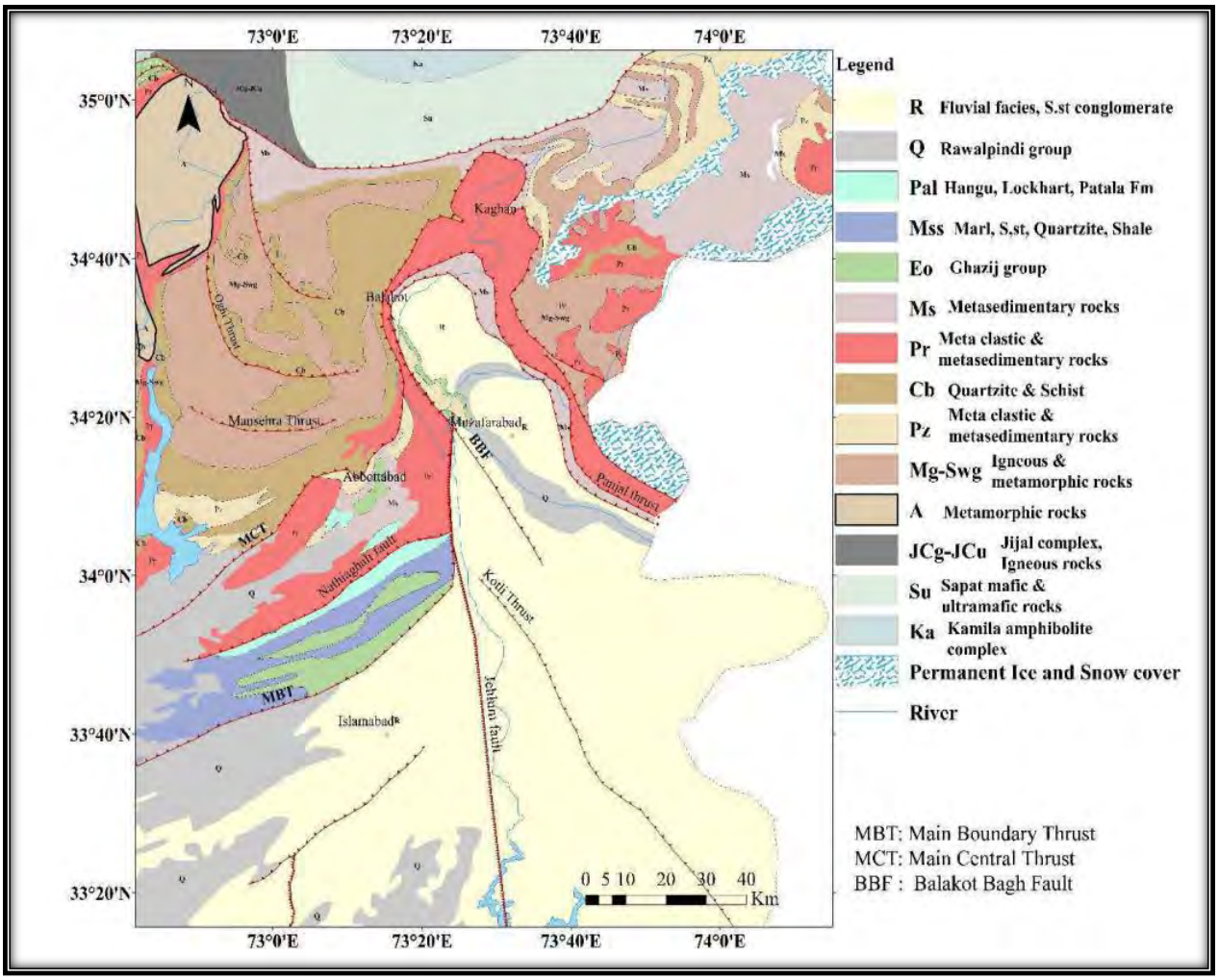

Figure 2.2:This is an illustration of Study Area's Seismo-tectonics (Khan & Searle, 1999)

MMT splits the KLA in the north into two parts: Kohistan to the east and Ladakh to the west, constituting the NP Syntaxis. The FMS map of seismic earthquakes along the Nanga Parbat Syntaxis reveals a NW to SE expansion, indicating that the NW Indian subduction zone is present here (Das & Pegler, 1998). Several geophysical investigations in the North-western Himalayas have already been conducted to examine the collision and subduction mechanism (Butler & Coward, 1985; Malinconico, 1989; Tiwari et al., 2009; Wallace & Fan, 1994). According to Koulakov and Sobolev (2006) and Ni et al. (1991) the Indian lithosphere dips gently to the northeast beneath the Himalayan arc, according to seismic tomography investigations of the NW Himalayas.

Other tectonic features include the Punjal-Khairabad Fault (PKF), which runs quite near to the Tarbela Dam. It is around 12 kilometres from the dam. It is thought to be 80 kilometers on the outer surface from the Hazara syntaxis, where it splays off the Himalayan thrust system, to the Attock area, when the former reunites the latter. Darband Fault (DF) is a left lateral strike slip fault with a severe dip that runs close beneath Tarbela Dam's main abutment, generating a 214 m near vertical escarpment in the dam foundation (Mahdi, 1988). The fault creates a steep gradient or escarpment perpendicular to the dam abutment. The fault line's total length is roughly 100 kilometers. Jehlum Fault (JF) also known as Balakot-Bagh fault is a strike-slip fault with a lateral extension between the towns of Balakot and Bagh in Azad Jammu & Kashmir. It is a NNW striking fault with a total length of over 100 km and is located roughly 70 kilometres from the Tarbela dam area and Fault in Rawalakot (RF) Tarbela Dam is 100 kilometres distant from the RF. It is a strike slip fault nearly 20-kilometer-long, with a northwesterly direction. It runs through 10 kilometres through Azad Jammu and Kashmir's Bagh city. According to Monalisa et al. (2005) the Khair-e-Murat Fault (KMF) is a 175 km long east-west trending feature. It progresses towards Kohat city parallel to the MBT, maintaining a distance of 20 -25 km till it reaches the capital, Islamabad, when it turns ENE and conceals or terminates behind quaternary deposits (Babar, 2014).

2.3 Gravity and Seismicity

Examining the seismicity of the MMT's eastern side in relation to certain geological features or geophysical anomalies was one of the goals of this study. The free-air anomaly is thought to be a representation of subsurface density contrasts. It is the most often used anomaly type in researches since it has the fewest assumptions and is used with surveys conducted at

constant elevation (Dehlinger, 1978). Previous researches revealed an association between free air gravity and dense seismicity, but it varies as per the topography of the region as well (Engen, Eldholm, & Bungum, 2003).

Coherence analysis between the Bouguer anomaly and topography is used to evaluate isostatic gravity anomalies and the effective elastic thickness (EET) of the lithosphere. The two main seismic zones in this region, the Indus-Kohistan Seismic Zone (IKSZ) and the Hindu Kush Seismic Zones (HKSZ), correlate to the isostatic residual gravity high and low, respectively. This suggests a relationship between seismicity and gravity anomalies. The Main Boundary Thrust's syntaxial bend, where high-density thrusted rocks are located, is the source of the gravity peak, which is also where crustal thrust earthquakes like the 2005 Kashmir earthquake have occurred. In the area of intermediate-deep focus earthquakes, where crustal rocks are underthrusting more quickly to form low density cold mantle, the HKSZ gravity low also occurs (Mishra,Tiwari, & Rajasekhar, 2009).

The presence of the Kohistan arc, which is associated with the well-known Indus-Tsangpo suture zone, between the Indian and the Eurasian plates, causes two sutures between them, namely the Northern suture between the Kohistan arc and the Eurasian plate and Main Mantle Thrust (MMT) between the Indian and the Kohistan arc.

Additionally, positive gravity anomalies are apparent over local topographic highs (thrust faults) and and topographic contrast, which induces differential shear stresses, can profoundly exert an influence on the process of deformational in the lithosphere (McKenzie & England, 1982).

As in the case of IKSZ, it appears that the region of gravity highs associated with thrusted high-density rocks may be active and producing thrust type earthquakes. IKSZ is much more hazardous since the underthrusting of the rocks on the north, east, and west sides may be putting extra strain on them and increasing their susceptibility to collapse. Additionally, the rocks underthrusting along the Main Frontal thrust in this area are connected to the Lahore-Sargodha ridge, which is characterised by gravity highs and high-density rocks, as well as the crustal bulge caused by the Himalayan load.

Due to the slab pull pressures that cause high-density rocks to underthrust more quickly and create greater strain, this area is more susceptible to seismic activity. The majority of earthquakes in IKSZ have focal depths of less than 50 km, which roughly corresponds to the effective elastic thickness in this region. This suggests that the entire crust is rigid, vulnerable, and capable of generating powerful earthquakes. The Sikkim Himalaya has also been observed to have an effective elastic thickness of 40 km (Tiwari et al. 2009), where seismic activity again corresponded with this zone.

High-density lower-crustal rocks appear to have been deposited in the upper portion of the major mantle thrust, and hypocenters of thrust earthquakes generally correlate with these high-density rocks and their assumed expansions depth-wise (Prasad & Verma, 1987).

Chapter 3

Data and Methods

3.1 Overview

Knowing the precise spatial offset between the earthquake hypocenters is necessary for seismicity analysis, which is used to research tectonic processes, earthquake recurrence, and earthquake interaction. This is especially true for crustal faults, which may be explored most easily utilizing microseismic activity. Studying the fine structure of seismicity is limited because the location uncertainty of routinely determined hypocenters is generally many times bigger than the source dimension of the earthquakes themselves (Waldhauser & Ellsworth, 2000). Relative earthquake localization techniques can also significantly reduce the effects of structural defects (Poupinet et al., 1984; Frechet, 1985; Fre'mont & Malone, 1987; Got et al., 1994).

Finding earthquake hypocenters has proven to be quite difficult. Many techniques have been tried out and used on many dataset worldwide. The Geiger method or "Single Earthquakes Determination (SED)" (Spence, 1980), "Joint Hypocenter Determination (JHD)" (Pujol, 2000; Kim et al., 2005), "HypoInverse" (Klein, 1989), and Double-difference method (Waldhauser & Ellsworth, 2000) are at least four well recognized earthquake relocation methodologies that are iterative as well as non-linear relocation. The smallest difference between the observed and theoretical arrival time is found using Geiger's approach, an iterative least-squares optimization (Maneno et al., 2019). The JHD approach, created by Douglas, A. (1967), increased earthquake localization accuracy based on seismic station calibration but was appropriate for small datasets. Further, location accuracy achieved by HypoInverse method which improves absolute location of earthquakes based on gradient descent. While HypoDD is a very high resolution double-difference hypocenter relocation method, which considerably improves the relative location of large dataset and reveals concentrated seismicity near earthquake source (Wu et al., 2022). The

HypoDD method calculates S and P wave travel-time difference dimensions among seismic stations from nearby earthquakes (Waldhauser & Ellsworth, 2000). The earthquake position might be successfully moved using this technique to the corresponding source. HypoDD assumes that two nearby earthquakes almost follow a similar path from source-receiver, which earthquakesually generates an identical waveform to a common station. The difference in arrival times for a couple of earthquakes noted on a common station is then adjusted to their locations; enable us to more precise earthquake's locations. In this thesis, we exploited the pros of body waves over the surface-wave that enables us to image the local small anomalies with high resolution, surface-wave capable to resolve only large-scale anomalies instead.

3.2 Source of Earthquake Data

The MSMS of the WAPDA Tarbela Dam Project, which consists of 19 local stations scattered across Northern Pakistan, has collected the earthquake data catalogue used, which spans the years 2010 to 2021 and includes 15561 occurrences with 162645 P wave and 29150 S wave arrival time phases. These earthquakes span in depth from 0.0011km to 800 km and have a local magnitude of M_L 2.0 to 7.72. In this study, the relative earthquake relocations were done using HypoDD earthquake relocation method (Waldhauser & Ellsworth, 2000). Seismic bulleting required for the hypocenter's relocation using HypoDD method consist of earthquake occurrence (origin time), initial hypocenter locations (lat, long, depth), the arrival time of body waves (S and P-wave) with minimum 4 observations per earthquake. In addition, the coordinates of stations are required. The combined 1-D velocity model is constructed which is comprised of Terbela (F-Model) and RID velocity model (Kennett and Engdahl, 1991). A standard Vp to Vs ratio, 1.73, has been chosen appropriate for earthquake relocations in study area (Figure 3.1).

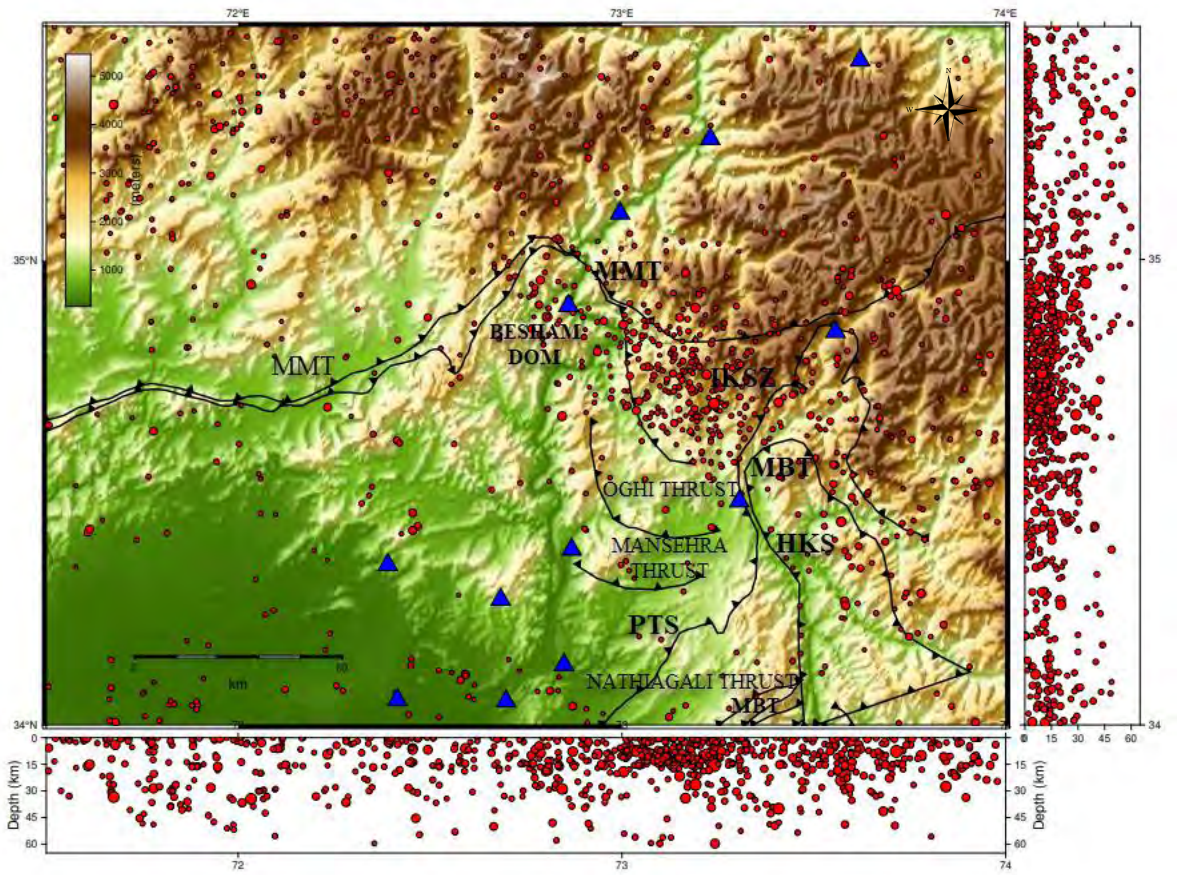

Figure 3.1: Distribution of sources and receivers, WAPDA-MSMS, used in this study where red circles show the seismicity recorded by the WAPDA-MSMS, and blue triangles show the locations of stations.

3.3 Double Difference (HypoDD) Algorithm

Earthquake site algorithms are typically centered on some variation of Geiger's technique, which involves linearizing the transit time equation by using Taylor's first-order series and connecting difference between the predicted and observed travel times to adjustments in the earthquakes' hypocenter coordinates for unknown (x, y, z, occurrence time) variables. Earthquakes can be located separately or jointly using this approach when other unknowns, like station corrections in the JHD technique or the earth crustal model (in seismic tomography); tie the responses to individual earthquakes. The HypoDD technique, which is thoroughly addressed in Waldhauser and Ellsworth (2000), can be employed if the distance between the earthquakes station and the separation between two hypocenters earthquakes is close to that distance. The ray

routes between the source region and a common station are comparable almost the whole length of the ray path, according to Frechet (1985) and Got et al. (1994).

In this instance, the spatial offset between the earthquakes can be accurately blamed for the variation in transit times for two earthquakes reported at the same station. HypoDD equations are an advance method in comparison to the equation for earthquake location developed by Geiger. Calculated and observed travel time residual of a same station between two earthquakes is linked with the changes in the hypocenter's relative position and origin time. By doing so, employing the travel time's partial derivative for every earthquake occurrence relative to the undetermined. HypoDD uses a layered velocity model to calculate trip lengths for the hypocenter at the station where the phase was collected. For each station, the SVD method and LSQR were used to minimize the double difference error for couples of earthquakes (Saunders & Paige, 1982).

After every iteration, the locations and partial derivatives were updated, and the vector difference between neighboring hypocentral combinations is changed to identify results. The receiver-side structure-specific common mode errors disappear by using the double-difference equations to linearized the earthquake location problem. Therefore, station changes or extremely precise projected travel times are not needed for the portion of the ray path that lies beyond the focus volume. When there are only a few hundred metres between subsequent earthquakes, or in places where seismicity is dispersed thickly, this strategy is especially useful.

Arrival time of body waves T from source i to seismic receiver k is defined using the path integral of ray theory,

$$T_k^i = \tau^{\,i} + \int_i^k \mathbf{u}\,\mathbf{ds} \ldots\ldots\ldots\ldots\ldots\ldots\ldots\ldots\ldots\ldots\ldots\ldots\ldots\ldots\ldots\ldots\ldots\ldots(1)$$

where i is the incident's origin time, u is the deliberateness area, and ds is a path vital component. The equation (1) is often solved using a truncated Taylor series expansion (Geiger, 1910) because the relationship between the starting time and the incident site is nonlinear. This oddity among the forecast and practical arrival times r_k^i linearly relates to the perturbation, Δm (x_1, x_2, x_3) and source times (τ), four hypocentral constraints for each observation k, and the velocity edifice parameters:

$$\frac{\partial t_k^i}{\partial \mathrm{m}} \Delta m^i = r_k^i \ldots\ldots\ldots\ldots\ldots\ldots\ldots\ldots\ldots\ldots\ldots\ldots\ldots\ldots\ldots\ldots(2)$$

$$r_k^i = \left(t^{obs} - t^{cal}\right)_k^i \ldots\ldots\ldots\ldots\ldots\ldots\ldots\ldots\ldots\ldots\ldots\ldots\ldots (3)$$

Equation (2) establishes a linear relationship between the travel time residuals (r_k^i), for a single earthquakes i and the perturbation vector (Δm^i), which is the modification of the travel time (t_k^i) and the hypocentral parameters like x, y, and z. Equation (3) the difference between the calculated (t^{cal}) and the observed travel time (t^{obs}) is known as the travel time residuals (r_k^i) (Fre´chet, 1985).

These formulas only apply to a single earthquake. There must be a connection between two occurrences for the double difference relocation to succeed.

$$\frac{\partial t_k^{ij}}{\partial \mathrm{m}} \Delta m^{ij} = dr_k^{ij} \ldots\ldots\ldots\ldots\ldots\ldots\ldots\ldots\ldots\ldots\ldots\ldots\ldots\ldots\ldots\ldots (4)$$

Equation (4) links relative hypocentral characteristics of pair of earthquakes denoted as i & j. The change in relative hypocentral parameters demonstrates this Δm_{ij}, (where $\Delta m_{ij}=\Delta x_{ij}$,

Δy_{ij} , Δz_{ij} , Δdt_{ij}).Partial derivative of travel time make up dr_k^{ij} (the slowness vector) which connects source to receiver (Aki & Richards, 1980)..

Differential travel times of pairs of earthquake by assuming a continual slowness vector, given by Thomson et al. (1987) in equation (5)

$$\boldsymbol{dr_k^{ij}} = \left(\boldsymbol{t}_{\boldsymbol{k}}^{\boldsymbol{i}} - \boldsymbol{t_k^j}\right)^{\boldsymbol{obs}} - \left(\boldsymbol{t}_{\boldsymbol{k}}^{\boldsymbol{i}} - \boldsymbol{t_k^j}\right)^{\boldsymbol{cal}} \quad \text{..... (5)}$$

By computing the discrepancy between the calculated and observed travel time for the two earthquakes denoted by i or j at station k, one can calculate the residual between them for any phase (P or S) (Figure. 3.2).

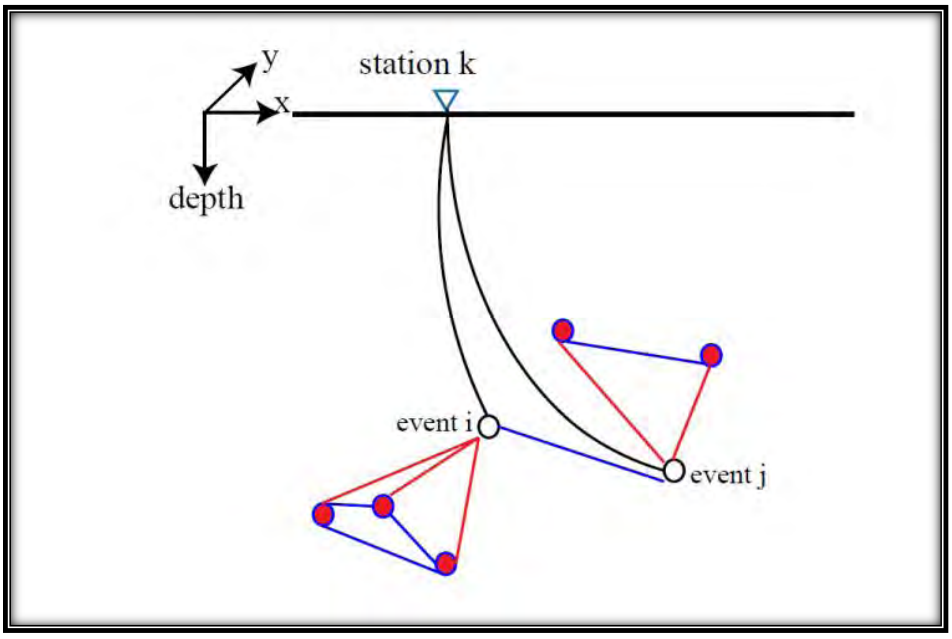

Figure 3.2: Illustration of Double Difference Algorithm

If the slowness is not constant, (Malone et al., 1987) then:

$$dr_k^{ij} = \frac{\partial t_k^i}{\partial x}\Delta x^i + \frac{\partial t_k^i}{\partial y}\Delta y^i + \frac{\partial t_k^i}{\partial z}\Delta z^i + \Delta t^i - \frac{\partial t_k^j}{\partial x}\Delta x^j - \frac{\partial t_k^j}{\partial y}\Delta y^j - \frac{\partial t_k^j}{\partial z}\Delta z^j - \Delta t^j \quad \text{.....(6)}$$

The origin time, t, and the hypocentral parameters x, y, and z are all represented. The residual travel times are determined by comparing the changes in each parameter for pair of earthquakes that. The equation becomes simple as:

$$dr_k^{ij} = \frac{\partial t_k^i}{\partial m}\Delta m^i - \frac{\partial t_k^j}{\partial m}\Delta m^j \quad \text{..... (7)}$$

The same parameters from equation (4) still hold; the ones being solved for are the hypo-central parameters, which are the origin time and position. According to Douglas et al. (1997) a system of linear equations can be created using equation (7). Thus, the system of linear equation is solved by:

$$WGm = Wd \text{..... (8)}$$

The partial derivatives are contained in the matrix G, which has a size of Mx4N and comprises the number of earthquakes N as well as the number of double difference observations M. The data vector, d, contains the double differences, and m now represents the change in origin and destination position. The diagonal weighting matrix will be utilized to weight each equation (Ellsworth &Waldhauser, 2000). Weighting matrix denoted by "W" is composed of predetermined arrival times phase pick quality. The P and S wave phases are equally weighted. Two methods—SVD and LSQR, are used to decrease the differential travel time residuals. Due to its inability to handle very large data sets, SVD can only be employed in small, well-constrained clusters. Moving large clusters or several clusters at once are no longer possible with SVD. The damped least squares problem is solved by LSQR (Saunders & Paige, 1982). The

strategy employed by Waldhauser and Ellsworth (2000) is to use a system of normal equations to find the weighted least squares solution, which is denoted by:

$$\left\| \boldsymbol{w}\begin{bmatrix} \boldsymbol{G} \\ \boldsymbol{\lambda I} \end{bmatrix} \boldsymbol{m} - \boldsymbol{w}\begin{bmatrix} \boldsymbol{d} \\ \boldsymbol{0} \end{bmatrix} \right\|_{\boldsymbol{2}} = \boldsymbol{0} \quad \text{.....(9)}$$

m still stands for the location and origin time that need to be calculated when employing LSQR, and I is denoted for identity matrix. The sparseness of the G matrix—caused by the fact that just two earthquakes are being linked together—is one of challenges in decreasing travel time residuals. The *G* matrix may become ill-conditioned if one earthquake is weakly linked to another, making the solution unstable when employing LSQR. Only allowing strongly linked earthquakes into the solution can solve this issue; however this becomes problematic with large sized dataset. By permitting damping of the solution, LSQR works with ill-conditioned systems; in equation, λ is the damping factor.

Effective earthquake migrations require a well-constrained regression problem solution. To test the sensitivity of input variables that influence HypoDD, such as "MAXSEP, WDCT, and DIST" are required for the evaluation of limitations and dependability. This is particularly true when collecting data from fewer than 10000 earthquakes, as it is challenging to establish well-connected earthquakes, and it is necessary to take into account weakly linked occurrences in order to find any solutions. The dataset used for this investigation is in this scenario.

3.4 HypoDD Program

Waldhauser and Ellsworth used the FORTRAN computer program package HypoDD to relocate during earthquakes (2001). HypoDD consists of two programs: (a) ph2dt for earthquakes pairing, and (b) HypoDD for relocating the earthquakes. The programs ph2dt and HypoDD, which compute the locations of double difference (DD) hypocenters, will be briefly

discussed in this subsection. It provides a brief introduction to the HypoDD method before discussing the pairing of earthquakes using ph2dt and the relocation of earthquakes using HypoDD. First, a brief introduction of phase based on their origin will be given, followed by the details of both programs (ph2dt and HypoDD).

Seismic Phases

The different wave types will be detected at seismic stations spread apart in time and may be divided at internal discontinuities because of the internal structure of the Earth (propagation velocities). Seismic phases are the beginnings of the several, distinct waves. One or more letters that each correspond to a distinct portion of the wave path are used to identify seismic phases (Figure 3.2). Upper case letters represent reflections through a boundary of the earth, while lower case letters imply reflections from a boundary. (such as P ,Pg S, Sg) .In this section, we will discuss about the different seismic phases, and how they are classified and their nomenclatures (Schweitzer et al., 2019).

Pg - Short-distance P waves that are either ascending from an upper crust source or levelling down there. Arrivals at greater distances are also a result of several primary wave reflections occurring throughout the entire crust at a cluster velocity of around 5.8 kilometers per hour.

Pn - Any primary wave that is bottoming in the topmost mantle or that is emitted from an uppermost mantle source. Most of its route is spent beneath the Moho barrier. Pn arrives at the recording station before Pg does for distances greater than 2°.

Sg - Like Pg, at close ranges, either an ascending S-wave from an upper crust source or an S-wave travelling upward to crust. Sometimes arrivals of S-wave reverberations at greater distances are converted into P wave.

Sn- Any S wave bottoming in the uppermost mantle or an up going S wave from a source in the uppermost mantle.

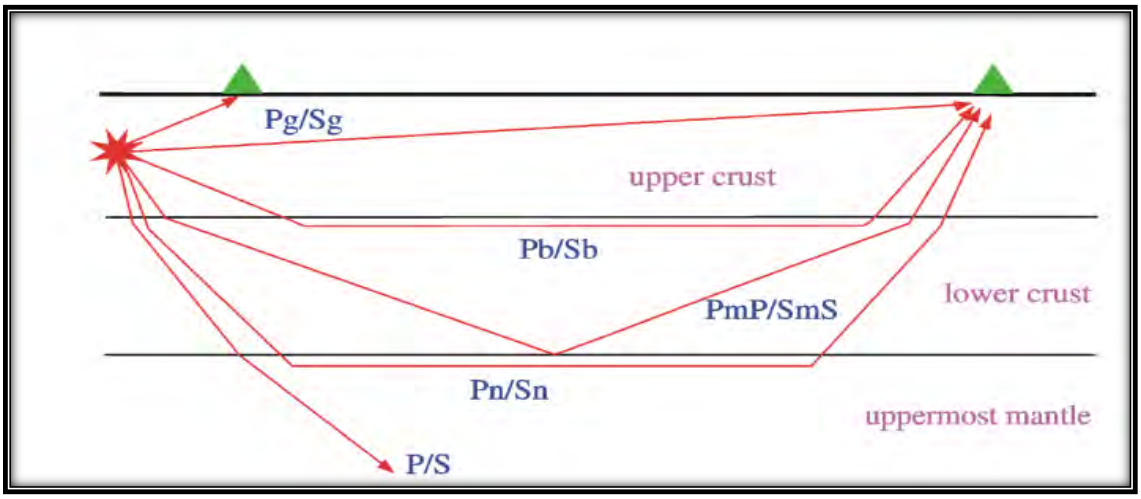

Figure 3.3: This illustrates body wave Crustal and Uper Mantle phases. Pg, Sg and Pn used in this research.

For combination of standard phase choices from earthquake-catalogues and to obtain high quality results then phase correlation of body waves may be used with the double-difference approach. In order to apply the same equation for both forms of data, the earlier type stated as "differential travel times". In order to connect all potential pairs of places for which data is available, travel time disparities are constructed (Pairing is discussed in more detail in section 3.4.1).Different data types and assessment levels of accuracy can be employed with dynamic preset standards to establish relative locations between multiplets, distances between pair of earthquake inside correlated clusters of earthquakes (multiplets), and statistically independent activities can be identified with the accuracy of list data.

HypoDD is completed in two steps to complete earthquake relocation process. To determine the travel times between two earthquakes, the analysis of waveform and/or catalogue phase data is the initial step. To improve the relationship between the earthquakes and reduce

outliers in the dataset, screening of the data is required. How to utilize ph2dt to process data from the catalogue phase is covered in detail in step two. Using the differential transit time data from step one, the positions of the double-difference hypocenters are established in the second phase. After ensuring that the group of vectors linking each earthquake to neighbors has no poor links that may cause significant numerical uncertainties, this procedure, carried out by relocation process of HypoDD.inp and detailed in section 4.2.2, solves for separation among hypocenters. The solution found by HypoDD needs to be rigorously evaluated, as is true for any least squares method, and the outcomes should not be blindly taken.

3.4.1 Formation of Pairs using Ph2dt

To determine the travel time of body waves, we utilize the difference between the earthquake's time of incidence and its time of arrival at certain locations (P- and S-wave phases). Following the same computation for all other occurrences in the seismic bulletin, we repeat the same process for each observation of a single earthquake. The information is then transformed into the necessary ph2dt format, which accepts hypocenter, and its travel time information is entered using the format given in Figure. 3.4.

```
1  # YR   MO DY HR MN SC     LAT     LON     DEP    MAG  EH EZ RMS ID
2  # 2010 03 10 09 27 30.441 35.4336 71.4419 7.9581 2.88  0  0  0  1
3  CHT          11.297    1     P
4  UTL          28.277    1     P
5  DAR          28.307    1     S
6  SWM          30.077    1     P
7  TAR          30.097    1     Pg
8  CAM          31.627    1     P
9  # 2010 03 10 08 52 13.744 35.4236 71.2929 13.5377 2.8  0  0   0  2
10 CHT          11.734    1     P
11 UTL          28.594    1     Sg
12 DAR          28.614    1     P
13 TAR          30.504    1     Pn
14 CAM          31.924    1     Sn
15 # 2010 03 11 14 59 23.123 34.1404 71.6699 12.0036 2.69 0   0   0  3
```

Figure 3.4:This Illustrates Format of Travel Time phase data required for input into HypoDD program.

According to Poupinet et al. (1984) travel time differences for pairs of earthquakes at similar stations make up the core data in HypoDD. Almost every seismic network will give earthquake catalogues, and this data can be retrieved from them or through waveforms cross-correlation In both cases, the minimum connectivity between earthquakes and the stability of the least squares solution need the trip time differences for pairs of earthquakes. The utility ph2dt, which generates input files for relocation of earthquake using HypoDD.inp from catalogue P-wave and S wave phase data, is discussed in this section.

To improve the precision in the process of phase pairing and the connection between the earthquakes, Ph2dt subsamples these statistics by searching the catalogue P- and S-phase data for earthquakes pairings at similar stations that include trip time information. A string of the pairwise connected earthquakes following from any one earthquake to other earthquakes, with the space between connected earthquakes being as short as is practical, would make up the ideal system of links between occurrences. By creating linkages from each earthquakes to as many MAXNGH nearby earthquakes as possible within the MAXSEP-specified search radius, Ph2dt creates such a network. Only "strong" neighbors are taken into account in order to obtain the maximum number of neighbors, or neighbors linked with phase pairs more than MINLNK value. Strong neighbors are chosen but not counted as "weak" neighbors, or neighbors with fewer phase pairs than MINLNK. Eight or more observations are often required to establish a solid relationship. Dataset consists of large numbers of observations for each earthquake pair do not, however, automatically imply a stable solution since, among other things, the distribution of the stations has a crucial impact on the solution. The nearest neighbour technique is used to identify neighbouring occurrences. This strategy works best when the earthquakes are dispersed randomly over the set criteria to search radius “MAXSEP” (i.e. if the value is equivalent to the

uncertainity in routine earthquake locations). In situations where seismicity is densely grouped in space across vast distances or if mistakes in beginning locations are lower than search radius, other methods, such Delauney tessellation, may be more suitable (Richard-Dinger and Shearer, 2000).

However, the search radius must not go above a geophysical significant value, in other words, two earthquakes hypocenter separation should be less than the earthquakes, stations and velocity variations. In many areas, a radius of around 10 kilometers is a good place to start. The number of potential double-difference observations (delay times), even with only a few hundred occurrences, may grow significantly.Limiting the number of connections for each earthquake pair or specifying a MINOBS and MAXOBS. of observations to be chosen for each earthquake pair, is one technique to get around this issue. Setting MINOBS equal to MINLNK allows one to only take into account tightly related earthquake pairings for a large number of earthquakes. With the following parameter settings, more than 10,000 well-connected earthquakes, for instance, Ph2dt would normally generate around one million delay times for example "MAXNGH = 6, MINLNK = 4, MINOBS = 4, MAXOBS = 20". On the other hand, one may choose every phase pair possible for a small number of earthquakes that form a close cluster by setting MINOBS assigned one, MAXOBS to the number of stations, and MAXNGH to the number of earthquakes.

A variety of vertical slowness values are needed to regulate the depth difference between earthquakes pairs. The depth offset between two earthquakes is often best controlled by stations adjacent to the earthquakes pair. Therefore, until the maximum number of observations per earthquakes pair (MAXOBS) is achieved, ph2dt chooses observations from increasingly far-off stations. Phase picks with pick weights less than MINWGHT but more than 0 are disregarded in

this process. Again, linkages between earthquakes pairings with fewer observations than MINOBS are disregarded. When the associated earthquakes additionally involve observations of this phase at the specific station, a negative weight is an indication of low quality data to ph2dt to include these values regardless of their absolute weight. When the diagonal element of the data resolution matrix, or Hat matrix, is greater than 1/2, the preprocessing software ncsn2pha automatically stamps reading weights with a negative sign. Users who lack important information are urged to think about preparing their input before sending it to ph2dt to flag critical station readings. Besides, the MAXOBS pairs that assign positive weight values to phases, readings with negative weights are also employed. Outlier observations are eliminated using Ph2dt. Delay periods that exceeds the maximum anticipated delay time for a certain earthquakes pairs are classified as outliers. The time it takes a primary and secondary waves to travel between two earthquakes is known as the maximum anticipated delay time, which can be computed using the original earthquakes locations and a P- and S-velocity in the focus region of 4 and 2.3 km/s, respectively. The cutoff is increased by assigning 0.5 seconds to accommodate for ambiguity in the initial positions. The file ph2dt.log contains information on outliers. The settings that regulate the outlier identification and removal task are programmed in ph2dt. However, it is simple to alter by changing the source code if necessary.

The number of weakly linked earthquakes, the average number of links per earthquakes pair, and the average distance between strongly linked earthquakes are three key values that indicate whether the earthquakes are generally well connected or not after the network of earthquakes pairs connecting all earthquakes have been established. The density of the hypocenter distribution is shown by the average distance between closely related earthquakes, which directs the selection of the maximum hypocenter separation permitted in HypoDD

(parameter WDCT, next section). To guarantee the stability of the inversion, HypoDD explicitly performs the clustering of earthquakes into well-connected earthquakes clusters (i.e., clusters where the earthquakes of one cluster never connect to the earthquakes of another cluster or only through earthquakes pairs with fewer than a predetermined number of observations) (see next section). The MAXNGH and/or MINLNK parameters in ph2dt can be adjusted to reach farther neighbours for each earthquake in order to promote connectivity throughout a cluster of earthquakes, but regrettably this comes at the expense of adding model errors during relocation. While raising MINLNK might pre-earthquakes ph2dt from locating MAXNGH neighbors within the search radius, increasing MAXNGH often results in longer delay periods.

It is advised to use data with a fair amount of latitude when using ph2dt and, if necessary, to apply extra restrictions while utilizing HypoDD (via OBSCT and WDCT). We refer to numerous current methodologies in order to acquire waveform-based differential arrival time measurements (e.g. Poupinet et al., 1984; Dodge, 1996; Schaff et al., 2005). Such information may be utilized alone in HypoDD or integrated with catalogue data with ease. But keep in mind that when using cross-correlation differential times, phases might only correlate for specific earthquakes-pair station arrangements, as when the earthquakes pair offset is close to the distance to a shared station and the focal mechanisms are very similar. Even while the measurements could be extremely precise, the spread of the partial derivatives may not be the best way to control the relative positions of the two earthquakes. The station arrangement needs to be examined before the move in order to assess the effects of the change.

Input Control File of Ph2dt.inp:

This file configures programme runtime parameters. Anywhere in the file will include a line beginning with "*," which is a comment line enter data in the following format (Figure 3.5).

```
* ph2dt.inp - input control file for program ph2dt
* Input station file:
Nstations.dat
* Input phase file:
*ph_dep_60.dat
TT_phase.dat
*MINWGHT: min. pick weight allowed
*MAXDIST: max. distance in km between event pair and stations
*MAXSEP: max. hypocentral separation in km
*MAXNGH: max. number of neighbors per event
*MINLNK: min. number of links required to define a neighbor
*MINOBS: min. number of links per pair saved
*MAXOBS: max. number of links per pair saved
*MINWGHT MAXDIST MAXSEP MAXNGH MINLNK MINOBS MAXOBS
   1      2000     20     6     4      4      6
```

Figure 3.5: Formate of ph2dt with input parameters required for the algorithm.

A ph2dt run generates the following five files “dt.ct, dt.cc, event.sel, event.dat, and ph2dt.log”. The ph2dt.log file records any stations that are not listed in the station list as well as the most recent ph2dt run and relevant data like weakly and strongly connected earthquakes. Catalog information and absolute travel times for chosen earthquake pair pairs are stored in the “dt.ct” file. If utilized, the dt.cc file records the differential travel time for earthquakes with cross-correlated waveforms. Both the selected earthquakes and all the earthquakes that were given access to the ph2dt software are recorded in “event.sel” and earthquakes.dat, respectively. HypoDD will make use of the files “dt.ct, dt.cc, and event.sel”; take note that “dt.cc” wasn't made or used and won't be either as cross-correlation data were just not employed in this study.

3.4.2. Relocating Earthquakes using HypoDD

The ph2dt software has been used to identify and record strongly connected earthquakes-pairs that may be used as input to HypoDD.inp file for relocations.

***Input Control File of HypoDD.inp**:*

In order to manage the program and adjust the computation to the unique properties of the data, this file specifies the parameter values. Anywhere in the file can contain comment lines, which are marked with a '*'. enter data in any format: Cross-correlation (cc) and catalogue (ct) are both abbreviations.

The example format with parameters is presented in Figure 3.6 Which shows the detailed properties of the relocation in a comprehensive way. Moreover, schematic diagram of some important relocation parameters are illustrated in Figure 3.7.

One-dimensional velocity model is the last input into HypoDD. The number of layers in this velocity model may go up to twelve. The input and fixed Vp/Vs ratio is used throughout the model. (One restriction of HypoDD is the use of a set Vp/Vs ratio. In every layer, the P wave velocity and layer thickness are allocated. In this study, the P wave travel durations are remained constant while the S wave travel times are modified by the Vp/Vs ratio, which is fixed at 1.73. The HypoDD input gives equal weight to the P and S wave phases.

The six files HypoDD.loc, HypoDD.reloc, HypoDD.sta, HypoDD.res, HypoDD.src, and HypoDD.log make up the output of the HypoDD software. The HypoDD.loc file contains the individual locations before relocations are conducted out. The HypoDD.reloc file displays the relocations in the similar way as the initial locations are done for comparison in visualizations tool such as Matlab. The HypoDD.sta file generates travel-time residuals at stations, whereas the HypoDD.res file generates differential times residuals. HypoDD.log offers the hypocentral take-off angles at station in addition to the input and control parameters.

```
* RELOC.INP:
*--- input file selection
* cross correlation diff times:

*
*catalog P diff times:
dt.ct
*
* event file:
event.sel
*
* station file:
Nstations.dat
*
*--- output file selection
* original locations:
V_LSQR_RID_MaxSep2000.loc
* relocations:
V_LSQR_RID_MaxSep2000.reloc
* station information:
V_LSQR_RID_MaxSep2000.sta
* residual information:
V_LSQR_RID_MaxSep2000.res
* source paramater information:
V_LSQR_RID_MaxSep2000.src
*
*--- data type selection:
* IDAT:  0 = synthetics; 1= cross corr; 2= catalog; 3= cross & cat
* IPHA: 1= P; 2= S; 3= P&S
* DIST:max dist [km] between cluster centroid and station
* IDAT   IPHA   DIST
 2     3     2000
*
*--- event clustering:
* OBSCC:    min # of obs/pair for crosstime data (0= no clustering)
* OBSCT:    min # of obs/pair for network data (0= no clustering)
* OBSCC  OBSCT
     0     0
*
*--- solution control:
* ISTART:   1 = from single source; 2 = from network sources
* ISOLV:    1 = SVD, 2=lsqr
* NSET:         number of sets of iteration with specifications following
*  ISTART  ISOLV  NSET
    2        2      2
*
*--- data weighting and re-weighting:
* NITER:        last iteration to used the following weights
* WTCCP, WTCCS:     weight cross P, S
* WTCTP, WTCTS:     weight catalog P, S
* WRCC, WRCT:       residual threshold in sec for cross, catalog data
* WDCC, WDCT:       max dist [km] between cross, catalog linked pairs
* DAMP:         damping (for lsqr only)
*        ---  CROSS DATA ----- ----CATALOG DATA ----
* NITER WTCCP WTCCS WRCC WDCC WTCTP WTCTS WRCT WDCT DAMP
  2     0.001 0.001   -9  -9  0.01  0.001  6   20   130
  2     0.001 0.001   -9  -9  1     0.1    4   6    130
*
*--- 1D model:
* NLAY:     number of model layers
* RATIO:    vp/vs ratio
* TOP:      depths of top of layer (km)
* VEL:      layer velocities (km/s)
* NLAY  RATIO
   4     1.73
* TOP
0.0   20   50  60
* VEL
* simplified RID MODEL
5.8 6.5  8.2  8.4
*
*--- event selection:
* CID:  cluster to be relocated (0 = all)
* ID:   cuspids of event to be relocated (8 per line)
* CID
    0
* ID
```

Figure 3.6: HypoDD format with input parameters required for relocation is presented.

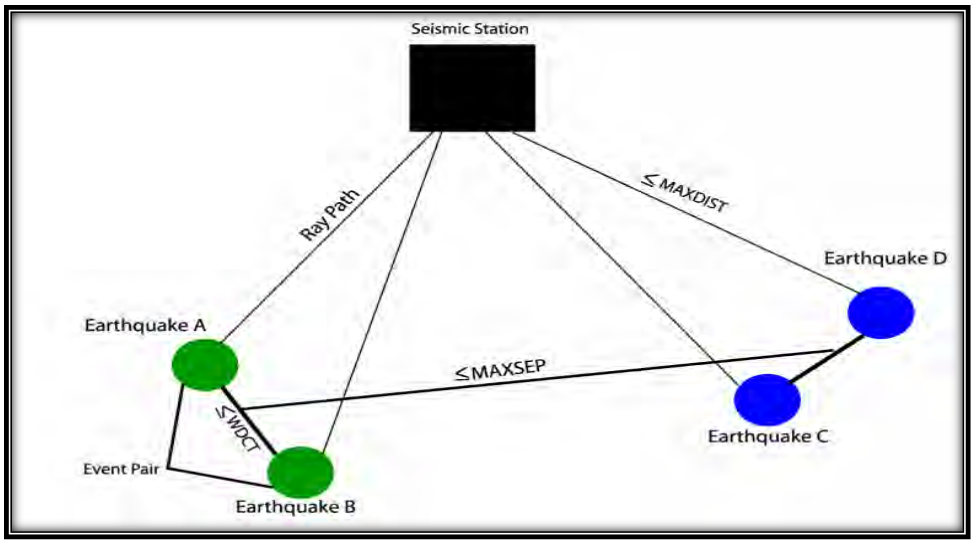

Figure 3.7: Schematic illustration of some important parameters of HypoDD Algorithms

3.5 Analysis of Solution Quality

The Double Difference results are worthless until some estimate of solution robustness or quality is made. The evaluation of the quality of model is based on two criteria: (1) improvement of misfits of travel-time residuals (2) Plausibility of hypocenter relocations.

3.5.1. Travel Time Residual Analysis

Distributions of travel-time residuals based on the 1D s model exhibits the travel-time residuals as function of epicentral distance before and after the inversion. Initial travel-time residuals have a non-Gaussian distribution ranging ±2 s, which reflects the implausibility of initial locations derived from the 1D velocity model. After inversion, the mean and standard deviation (σ) of travel-time residuals is significantly reduced to about ±0.5s or less. The 1D model achieved a significant reduction in travel-time residuals such a reduction from the initial model to the final model indicates the robustness of obtained results and the precise relocation of the earthquakes (Riaz et al., 2017).

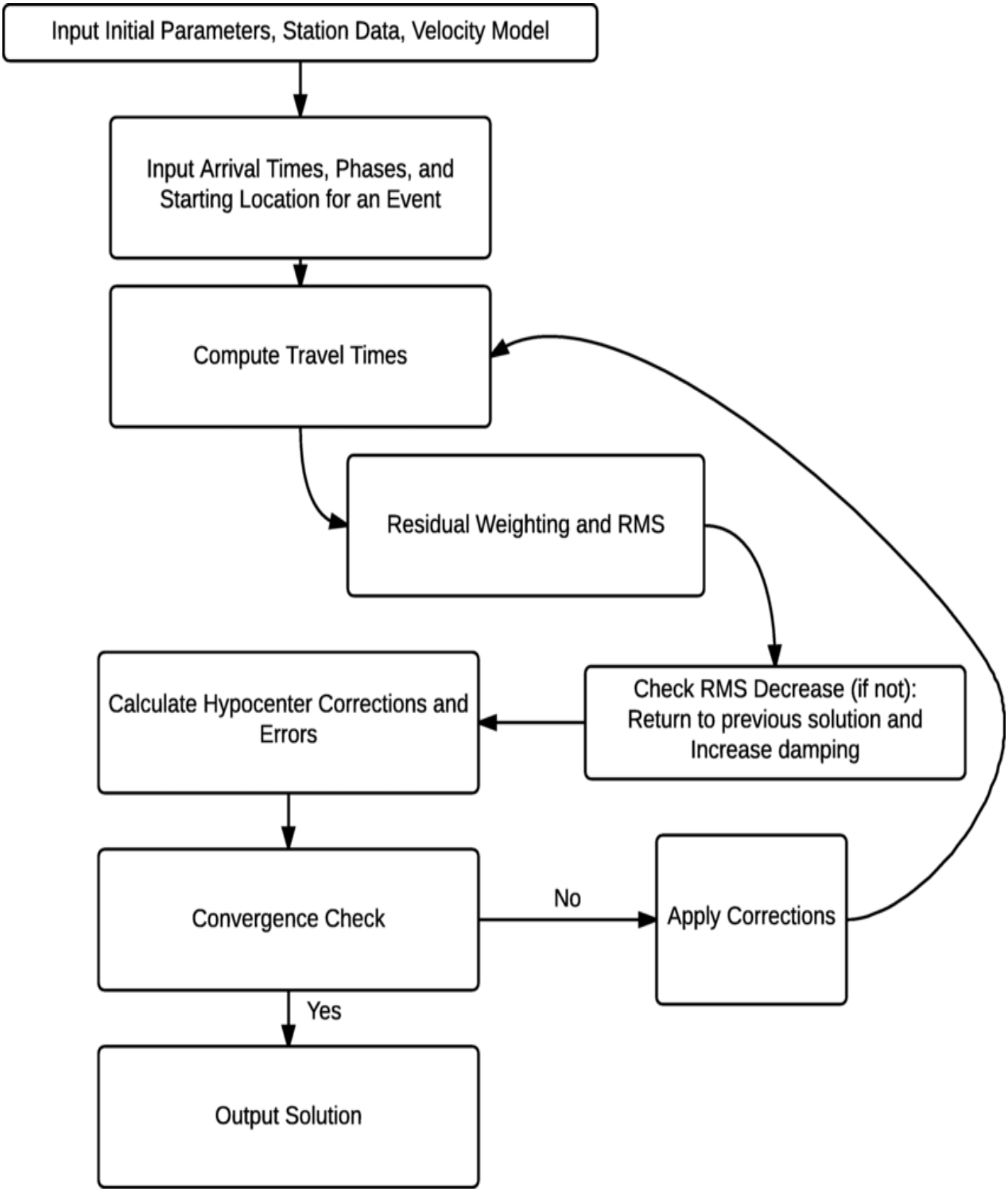

Figure 3.8: This Flowchart illustrates the various steps involved in HypoDD Method to complete the Study (Turquet et al., 2019)

3.6 HypoDD Application in NW Himalayas

The analysis procedure of Double difference relocation (HypoDD) algorithm described (Figure 3.8) will be applied to the seismically active NW Himalayas especially in Indus Kohistan Seismic Zone (IKSZ). Identifying potential seismogenic fault sites and orientations in our study region is one of the objectives of our research. The technique is then used to earthquake phase data for the years 2010 through 2021 obtained from the network of the WAPDA-MSMS Terbela catalogue. After preprocessing, hypocenter relocations and 3D depth profiles are generated using HypoDD algorithm, the comparison of seismic data from before and after the relocation is then examined. Further, the reliability of relocated hypocenter results are assessed by travel time residual analysis. Lastly, results derived from double difference method are correlated with FMS and gravity to achieve objective of this research.

Chapter 4
Results and Discussion

4.1 Overview

The research was carried out to study earthquake relocation and investigation of seismogenic structures of NW Himalayas through HypoDD method, FMS, and Gravity method. Appropriate hypocentral input parameters were set to conduct the computational procedures. After that, data were cleaned, and reliability was computed by travel time residual. To relocate earthquakes' large system of nonlinear observations, the HypoDD opted the LSQR algorithm with a damping regularization inversion strategy was used iteratively. Moreover, the results of both hypocentral location estimated by WAPDA and relocation calculated through HypoDD method were compared. Cross-sections were constructed to analyze seismicity distribution, fault orientations and seismogenic environment specifically in IKSZ. Lastly, results derived from double difference method are integrated with FMS and gravity method which obtained results by EGM2008 model to achieve the objective of this research.

4.2 Data and Inversion Strategy

The phase report of P- and S-wave arrival times of local earthquakes is used in the study recorded by WAPDA Network (Figure. 3.4). The average uncertainty for body wave arrival times is assumed about ±2.0 s. First, 15561 total numbers of earthquakes were collected with $M_L \geq 2.0$ that occurred from 2010 to 2021. Then, the study selected the higher quality data by imposing two requirements: (1) Earthquakes having at least four observations with a hypocentral distance of 2000 km, were chosen and (2) Residuals of travel times must be $\pm \leq 2.0$ s. After that algorithm obtained earthquakes recorded by selected seismic stations consists of 11703 matched differential travel times. The average number of observations per earthquakes is 4.

In the present study 186150 differential travel times for earthquakes pairs having a maximum hypocentral separation of 20 km, with 130043 P-wave and 56107 S-wave travel times were computed (Figure 4.2). An accurate reference crustal velocity model is essential to obtain robust results. Due to the structural heterogeneities of the region under study, a simple 1-D velocity model may not be suitable. To overcome the limitation of a single local 1-D model, an average simplified 1-D model is built by analyzing residual results during processing by local Terbela and regional 1-D models (Table 2, 3). The differences between these models are mainly at the Moho depth as Terbela reported 33 km while regional estimated 60 km. fortunately, these differences are within the range of uncertainty of any model in the study area. In final simplified model, the Moho's depth ranges up to 60 Km (Johnson & Vincent, 2002).

In addition, to the reference velocity model, initial Vp/Vs ratio is also of equal importance which is 1.73 as reported by WAPDA MSMS. Then, the inversion performed in a LSQR method normalized by damping 130 to obtain optimal CND. Following the methodology of HypoDD, a hierarchical weighting scheme to the differential data. In the first five iterations, the P differential data were weighted by a factor of 10 times more than the S differential data to compute earthquakes relocations. The conditions applied is to yield result over final iterations, where RMSCT up to 79 ms, CND up to 44 and airquakes should decreased up to 0 (Figure 4.1). Final iteration of the inversion discarded 153 airquakes which were above surface. The horizontal, vertical and depth direction initial position of were 1174 m, 733 m, and 2707 m respectively, while after relocation final position were 145 m, 98 and 89 m. The RMS residual reduced from 155 ms to 79 ms. Thus, more precise 6373 relocated earthquakes plotted in the study region (Figure 4.4 & 4.5).

Table 1

Ph2dt Input Parameter for Earthquakes Pairing.

Parameter	Input Value	Parameter	Input Value
MINWGHT	1	MINLNK	4
MAXDIST	2000	MINOBS	4
MAXSEP	20	MAXOBS	6
MAXNGH	6		

NOTE. MINWGHT= min. pick weight allowed, MAXDIST= max dist (km) between event pair and stations, MAXSEP= max hypocentral separation in km, MAXNGH= max no. of neighbors per event, MINLNK = min no. of links required to define a neighbor, MINOBS = min no. of links per pair saved, MAXOBS = max no. of links per pair saved.

Table 2

HypoDD Input Parameters for Earthquakes Relocation

Parameter	Input Value	Parameter	Input Value	
		NSET 2 times		
IDAT	2	NITER	2	2
IPHA	3	WTCTP	0.01	1
DIST	2000	WTCTS	0.001	0.01
OBSCT	0	WRCT	6	4
ISTART	2	WDCT	20	6
ISOLV	2	DAMP	130	130
CID	0			

NOTE. IDAT= data type, IPHA= p&s phase type, DIST= max distance (km) between cluster centroid and station, OBSCT, min # of obs /pair for network data, ISTART= solution control from network sources, ISOLV= LSQR, CID= cluster to be relocated, NSET= no. of set of iteration, NITER= last iteration to used, WTCTP= weight catalog P, WTCTS= weight catalog S, WRCT= residual threshold in sec for catalog data, WDCT= max dist (km) between catalog linked pairs, DAMP= damping.

Table 3

HypoDD Input Velocity Model (Johnson & Vincent, 2002).

Layer No.	Depth to the Top of Layer (Km)	P Wave Velocity (km/s)
1	0.000	5.800
2	20.000	6.500
3	50.000	8.200
4	60.000	8.400

Note: Vp/Vs ratio is 1.73 used in the velocity model.

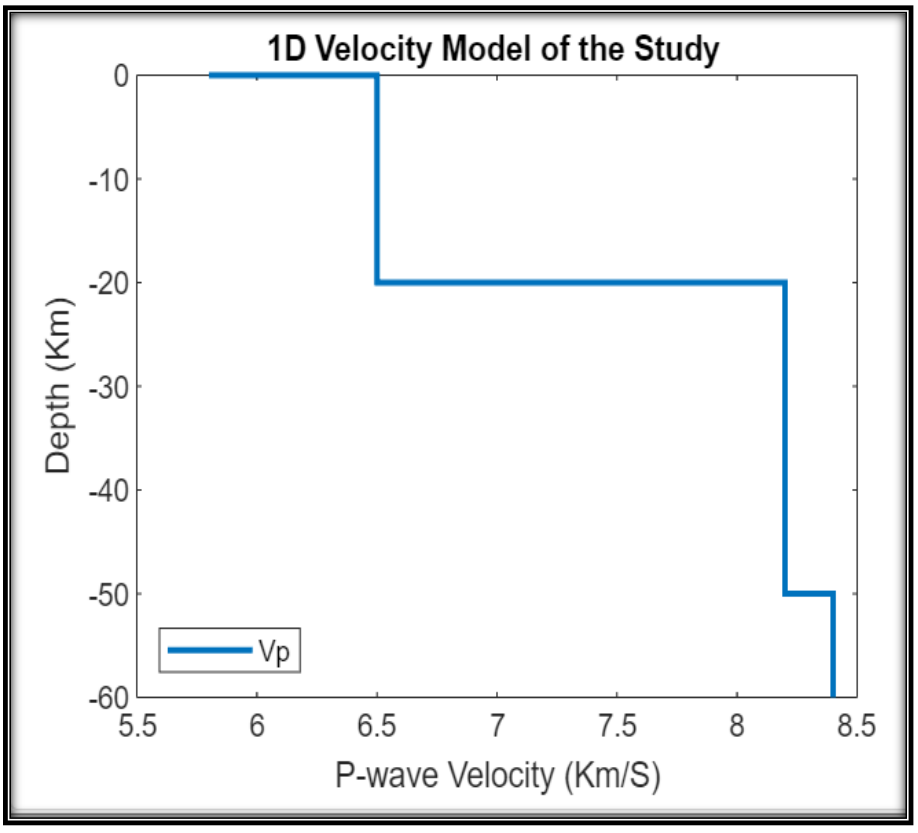

Figure 4.1: Simplified Input RID Velocity Model (Johnson & Vincent, 2002)

```
INPUT FILES:
cross dtime data:
catalog dtime data: dt.ct
events: event.sel
stations: Nstations.dat
OUTPUT FILES:
initial locations: V_LSQR_RID_MaxSep2000.loc
relocated events: V_LSQR_RID_MaxSep2000.reloc
event pair residuals: V_LSQR_RID_MaxSep2000.res
station residuals: V_LSQR_RID_MaxSep2000.sta
source parameters: V_LSQR_RID_MaxSep2000.src
 Relocate all clusters
 Relocate all events
Reading data ...   Sat Feb 11 17:26:43 2023
# events = 15561
# stations < maxdist =     29
# catalog P dtimes =  130043
# catalog S dtimes =   56107
# dtimes total =   186150
# events after dtime match =      11703
# stations =     25

no clustering performed.

RELOCATION OF CLUSTER: 1     Sat Feb 11 17:26:44 2023
---------------------
Initial trial sources = 11703

  IT   EV  CT    RMSCT   RMSST   DX   DY   DZ   DT   OS  AQ  CND
       %   %   ms     %    ms    m    m    m   ms    m
 1     99  91  154 -28.1     0 1161  724***** 35    0 140  102
 2     97  89  145  -6.0     0 1046  622 2811 29    0  36   99
 3     96  88  143  -1.5     0 1051  608 2540 28    0   5   99
 4     96  88  143  -0.3     0 1016  606 2207 28    0   2   99
 5  1  96  88  143  -0.1   579 1015  605 2212 28 1183   0   99
 6     93  84  130  -9.0   579  582  333  677 13 1183  23   93
 7  2  93  83  127  -1.8   256  570  325  502 12   44   0   93
 8     56  33  102 -20.0   256  248  159  143  5   44   3   48
 9  3  56  31   87 -14.8   159  226  147  129  5   84   0   48
10     55  29   71 -17.9   159  133   92   82  2   84   1   44
11  4  55  28   66  -8.0   123  128   89   79  2   83   0   44
```

Figure 4.2: The data demonstrates the output log of HypoDD.

4.3 Quality of Results by Residual Analysis

We evaluate the quality of the model based on two criteria: (1) improvement of misfits of travel time residuals, (2) Plausibility of hypocenter relocations.

Distribution of travel time residuals based on the 1-D velocity model are shown (Figure 4.3). This residual histogram exhibits the frequency of earthquakes as a function of residuals after the inversion done by HypoDD algorithm. Furthermore, the travel time residuals have a Gaussian distribution ranging ±0.8 s, which reflects the plausibility of hypocenter relocation (Figure 3.4). After inversion, travel time residuals are significantly reduced up to 28% and such a reduction from the initial model to the final model indicates the robustness of obtained the precise relocation of the earthquakes. The initial horizontal, vertical and depth direction position were 1161 m, 724 m and 2811 m respectively while after relocation horizontal, vertical and depth position were 128 m, 89 m and 79 m. The RMS reduced from 154 ms to 66 ms and RMSST error at station also decreased from 504 m to 181 m.

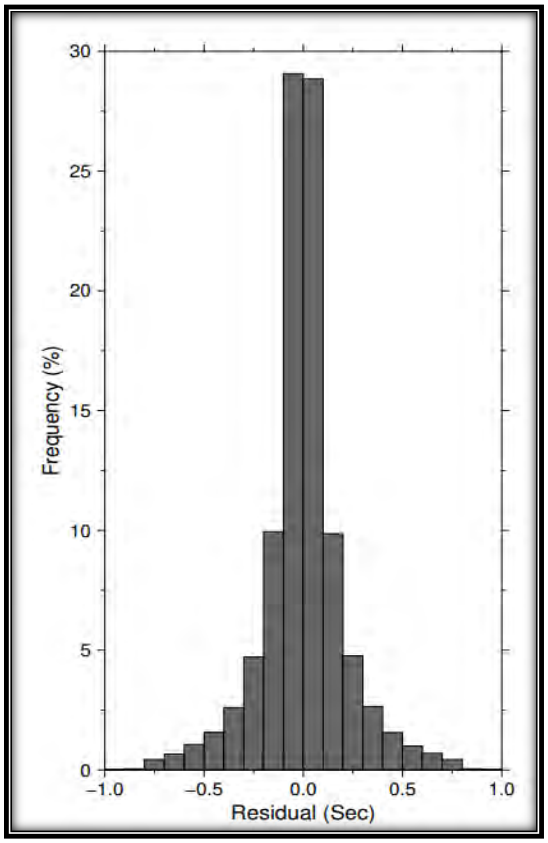

Figure 4.3: Illustrates Robustness of Results with the help of Residual Histogram

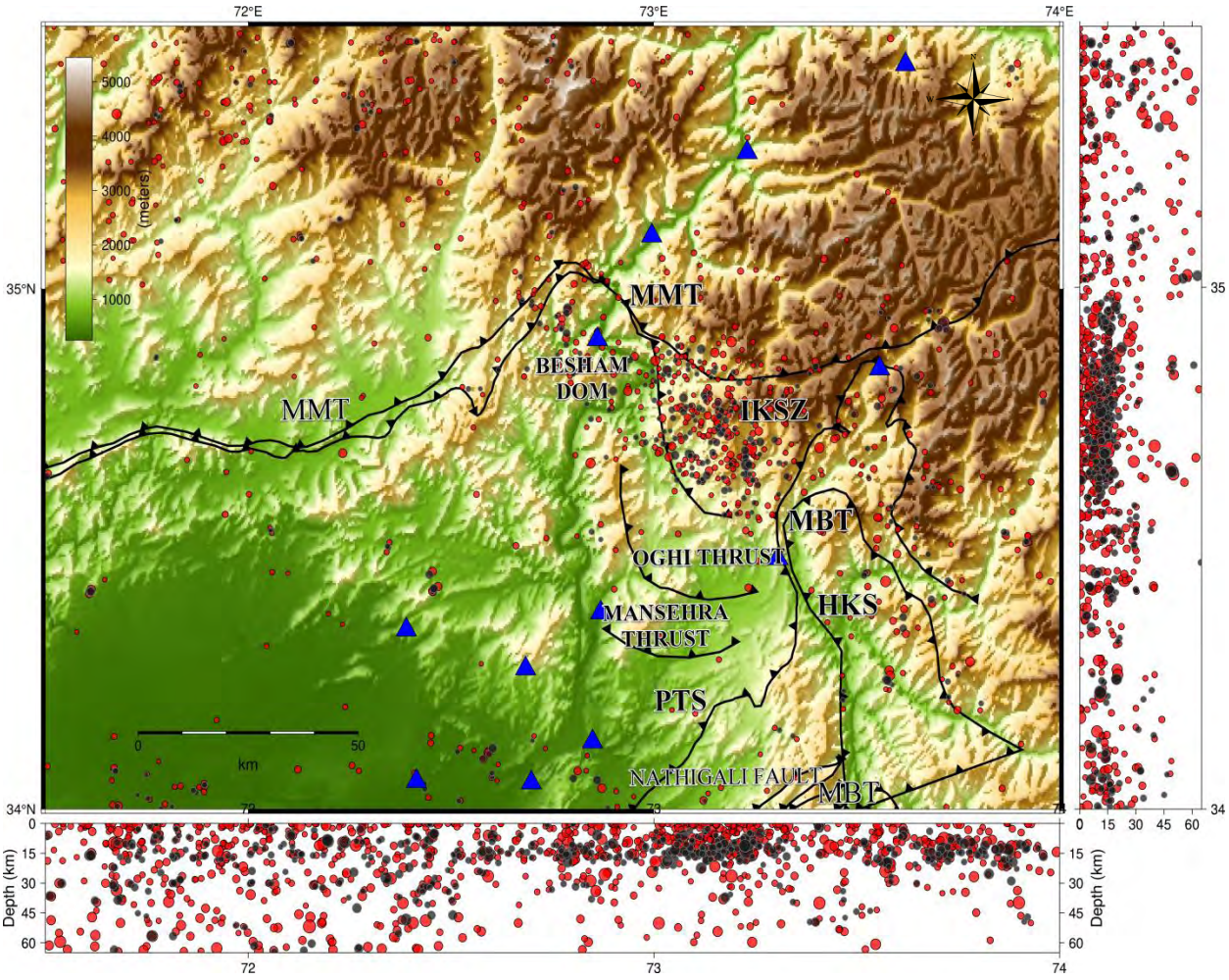

Figure 4.4: Map illustrates the orignal location(red circles) and relocation(grey circles) of seismicity with station distribution(blue triangles) wid major tectonic s and topography of study area.

In figure 4.4, the original hypocenters of each earthquake, their estimated focal depths from WAPDA, and the relocations from HypoDD are superimposed. Red color shows the distribution of earthquakes before relocation and grey color shows the distribution of earthquake source after relocated using hypoDD. The distribution of earthquake sources to the collecting depths forms two clusters at 0-20 km dept between 73^0E - 74^0 E, 34.5^0N - 35.0^0N. The displayed map illustrates the clustered areas are changed. Seismicity distribution after relocation has more clustered pattern in IKSZ.

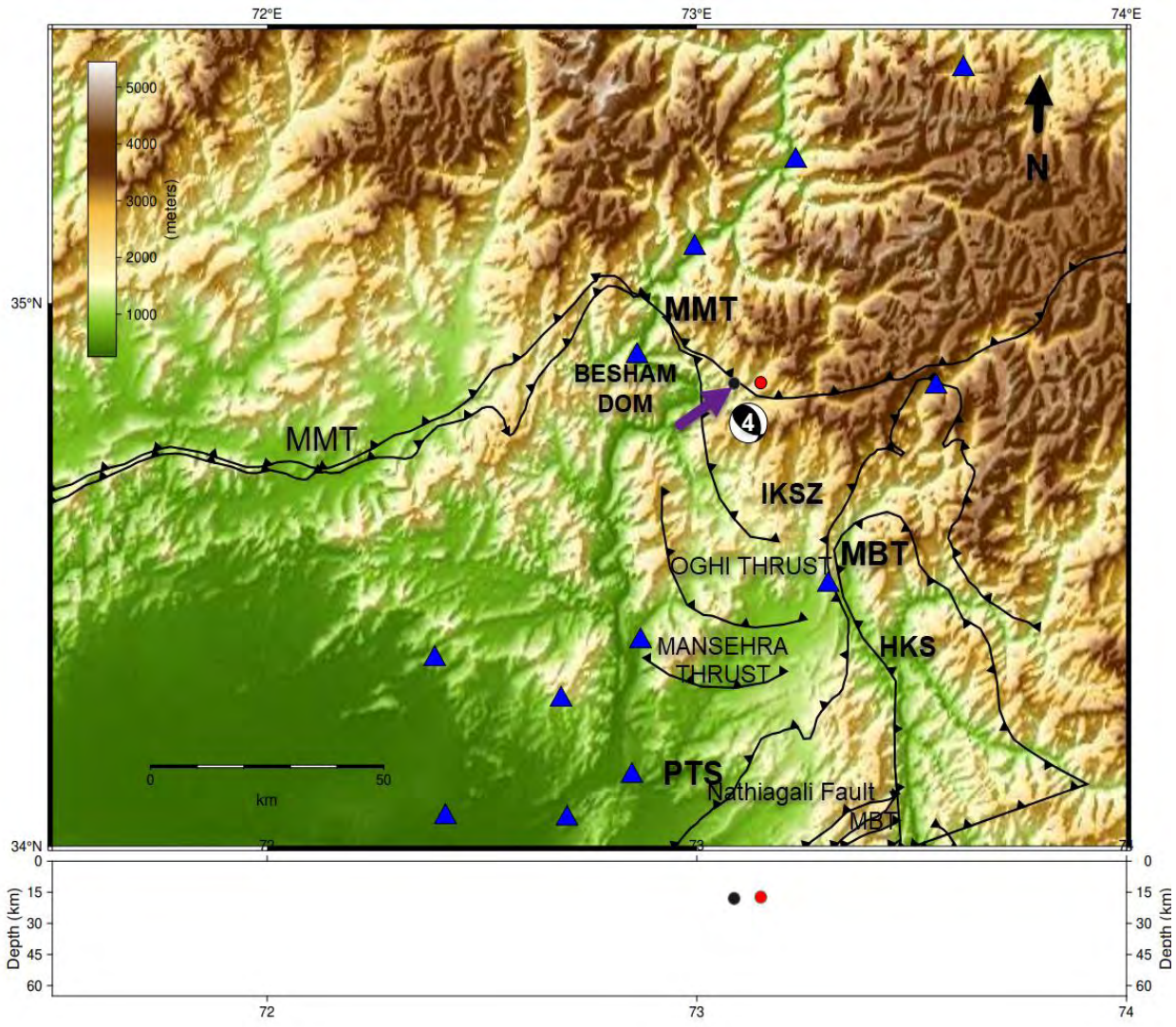

Figure 4.6:The Map illustrates the single event relocation along the MMT with FMS. Red circle shows original location estimated by WAPDA and grey circle denotes relocated earthquake by HypoDD.

The HypoDD algorithm's affectivity for earthquakes relocation is illustrated on the above map (Figure 4.5). After the relocation the depth of earthquake tends to located slightly deeper and more precisely follow the seismogenic structure MMT (Figure 4.5). In addition to, change in hypocenter positions (x, y, z) and reduction in errors (residual) are demonstrated numerically in output log (Figure 4.2).

Table 4

Focal Mechanism Solutions of Study Area

Sr. No	Date (Y/M/D)	Latitude (°N)	Longitude (°E)	Depth (Km)	M_w	$Strike_1$ (°)	$Strike_2$ (°)	Dip_1 (°)	Dip_2 (°)	Fault Type
1	1981/09/12	35.22	73.48	10.0	6.1	107°	300°	36°	54°	Thrust
2	1982/02/22	35.15	73.40	15.0	5.2	123°	322°	43°	48°	Thrust
3	2004/02/14	34.75	73.22	12.0	5.4	111°	336°	49°	122°	Thrust
4	2004/02/14	34.78	73.12	19.0	5.3	339°	123°	40°	56°	Thrust
5	2005/10/08	34.38	73.47	12.0	7.6	334°	114°	40°	57°	Thrust
6	2005/10/08	34.70	73.12	12.0	6.4	328°	127°	39°	53°	Thrust
7	2005/10/08	34.58	73.06	14.3	5.6	321°	121°	31°	60°	Thrust
8	2005/10/08	34.62	73.34	17.2	5.7	96°	321°	47°	53°	Thrust
9	2012/08/13	34.80	73.75	18.1	5.0	239°	7°	38°	65°	Thrust
10	2015/02/26	34.57	73.28	19.7	5.1	301°	125°	37°	53°	Thrust
11	2016/10/01	34.82	73.54	16.9	5.1	219°	37°	36°	54°	Thrust

Note. *Strike1, strike 2 and Dip1 and Dip2 crosspond to fault planes strikes and dip angles.*

In the study area (34°N-35.5°N, 71.5°E-74°E) (Figure 4.6), 6426 earthquakes with minimal travel time residuals of <1 s have been found for earthquakes relocations. Twenty-five recording stations were employed during processing to generate results for this study. A suitable hypocentral distribution of earthquakes with residual less than1 s was achieved after deleting the occurrences gradually with travel duration residual > 1 s. Figure 4.4 shows that compared to the original locations predicted by the WAPDA, the earthquakes were well concentrated after they were relocated (Figure 4.6).

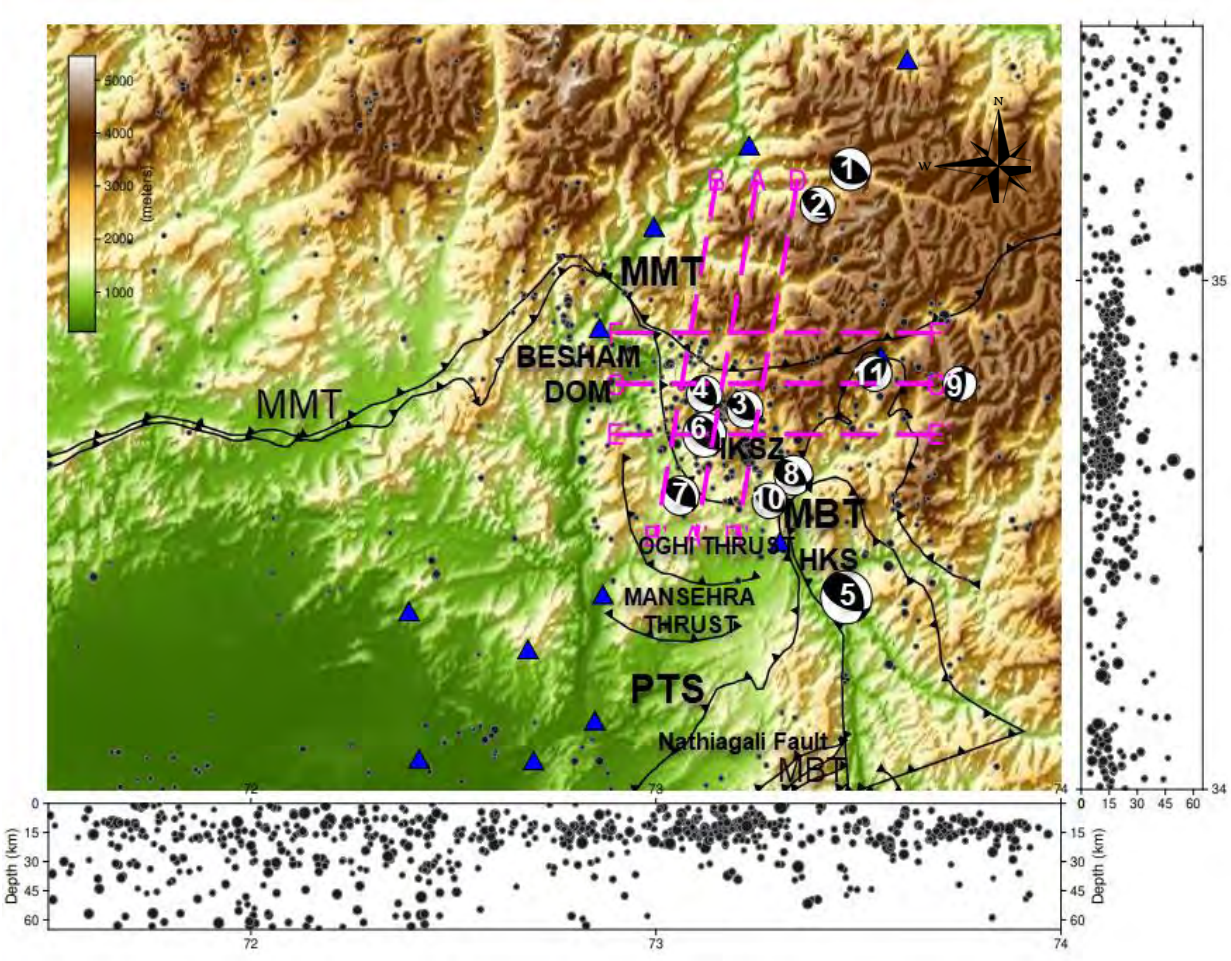

Figure 4.6: This illustrates relocated seismicity distribution, FMS (www.GCMT.org) distribution and cross-section with regional tectonics and topography.

In the studied area, the clusters of the seismicity are localized in the shallow crustal depth range from 5 to 30 km. Only a couple of earthquakes, one in the Hindu Kush region while the other in the IKSZ, were discovered at depths greater than 40 km. As a result, earthquakes at shallow depth were moved to a depth of 5 to 30 km, deep earthquakes to a depth of 50 km, and deeper earthquakes range from 50 to 60 km. The new study's assessment of the depth of earthquakes in this region is similar with earlier investigations (Ni et al., 1991). In Northeastern side of MMT, the IKSZ has a higher seismicity than the nearby zones. While the relocation of the hypocentral distribution of earthquakes from 2010 to 2021 was depicted in Figure (4.5, 4.6) alongside significant tectonic structures and seismic sources, the reactivation of MMT features

was connected with shallow crustal seismicity. Additionally, these relocations were contrasted with those calculated by WAPDA.

The 100 kilometer long and 50 kilometer wide IKSZ was described by Armbruster and Seeber (1979) using the micro-seismic data collected at Tarbela and Chashma seismic networks and according to the their study, most seismic activity in IKSZ is restricted to depths of 5 to 25 km, but some earthquakes have been generated at depths of up to 70 km.. According to the current current study in Figure 4.5, seismicity distribution in the research area is concentrated in four different clusters after the relocation of seismic earthquakes. Cluster 1 in Hazara Kashmir Syntaxes is along the Punjal Thrust. Cluster 2 associated with IKSZ, Cluster 3 is along the Besham dome, and Cluster 4 is along northeast to southwest trending MMT and the similar results are suggested in previous studies (Khurshid et al. 1984).Based on seismicity distribution pattern, seismogenic sources, seismo-tectonic zones, and earthquake relocation, these four clusters represent the distribution of earthquakes in the vicinity of MMT.

Moreover, IKSZ has three sub-clusters of seismicity that are all oriented northeast-southwest: a shallow zone up to a depth of 10 km (Figure 4.7); a mid-crustal zone between a depth of 10 and 25 km (Figure 4.7); and a deeper zone below a depth of 25 km (Figure 4.8).

These zones help to infer the existence of blind faults that have not yet been identified and properly mapped as previous studies suggested similar results. These problems are typically found close to the plate boundaries. These sources are known to cause earthquakes termed as blind thrust earthquakes. High compressional stresses are present during the development of these faults. Since these faults are not visible from the surface and a zone of diffuse seismicity is present at a depth of around 40 to 50 km, this demonstrates that the Indian Plate is experiencing intra-plate activity. While the deeper seismicity may be due to the Indian plate pushing beneath

the IKSZ, which serves as the principal thrust zone, the near surface seismicity is assumed to be related to the reactivation parts of the MMT.As in the IKSZ, two significant earthquakes such as Pattan occurred in1974 and Kashmir occurred in 2005—were already predicted (Khurshid et al. 1984; Mona et al. 2008) however, we suggested that the earthquakes in Kashmir and Pattan can be divided into two clusters which help to confirm the source of the Pattan and Kashmir earthquakes is considered the IKSZ as proposed in previous studies.

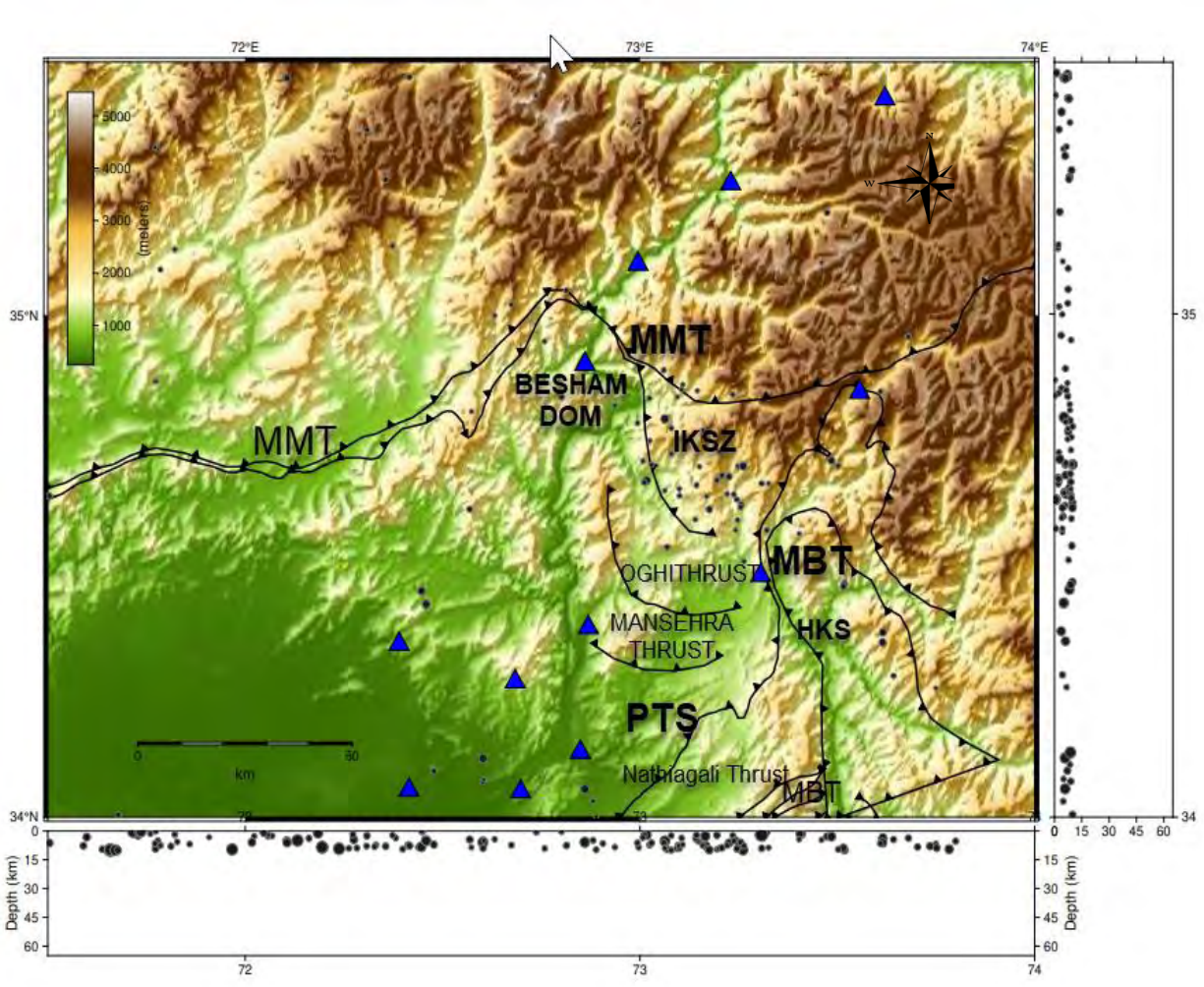

Figure 4.7: Map illustrates shallow zone in IKSZ of relocated seismicity from 0_10km depth.

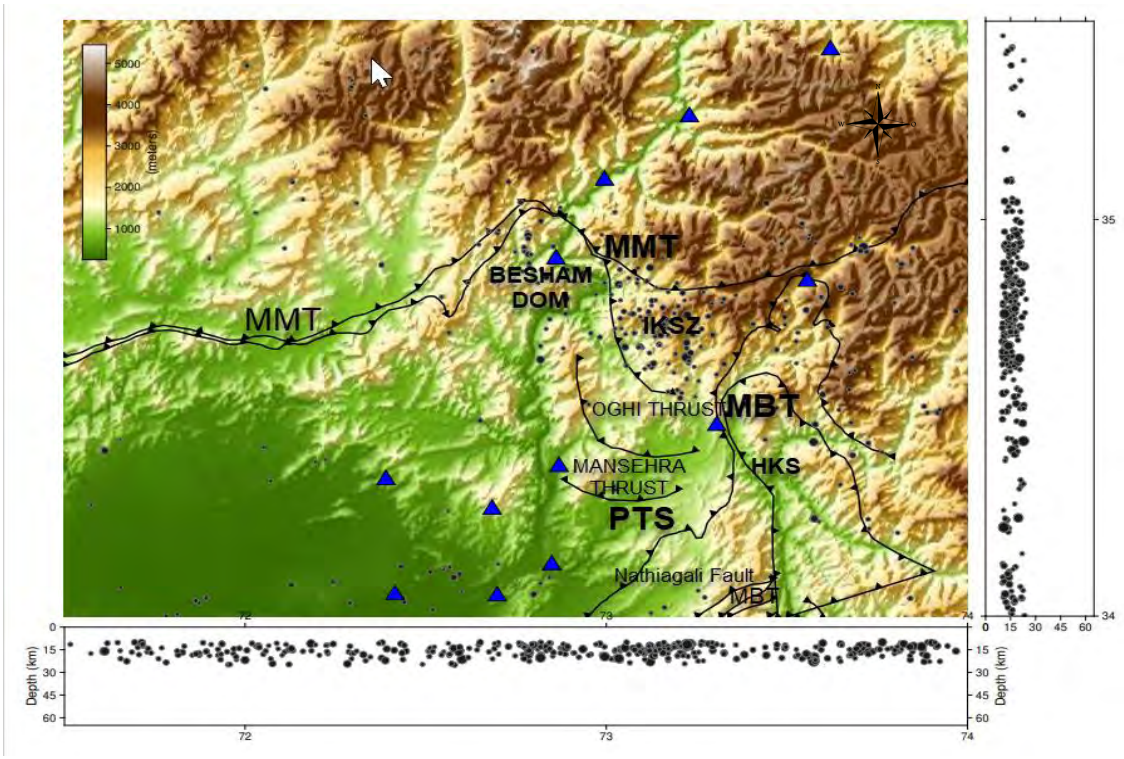

Figure 4.8: Map illustrates shallow zone in IKSZ of relocated seismicity from 10_25 km depth.

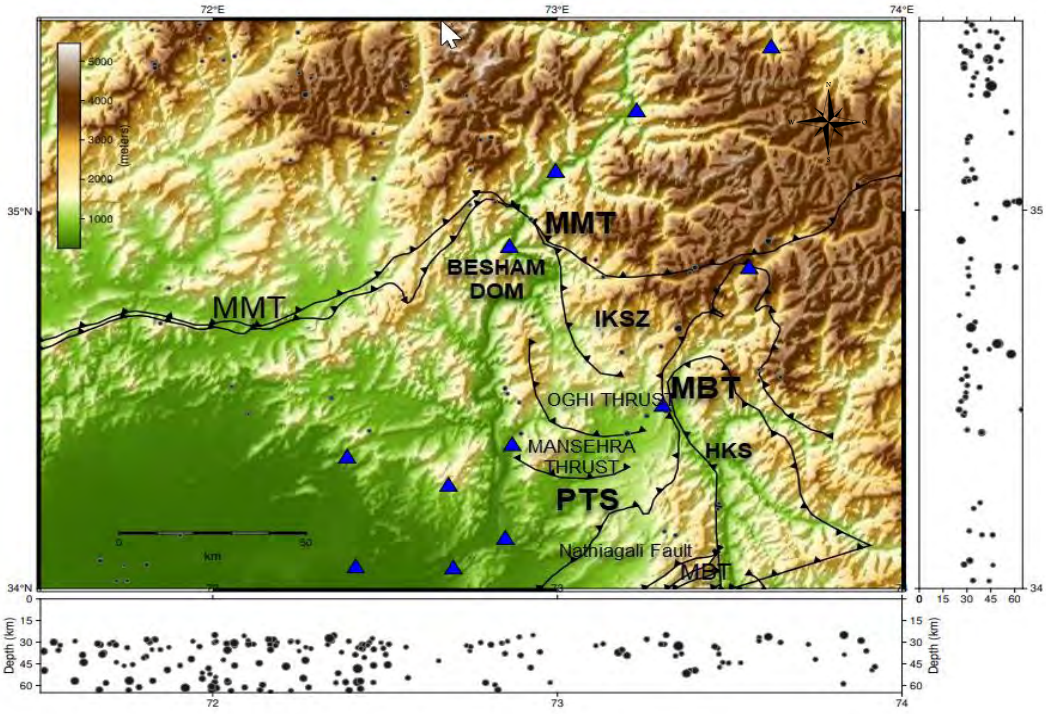

Figure 4.9: Map illustrates shallow zone in IKSZ of relocated seismicity from greater than 25 km depth.

To explore the correlation between relocated seismicity and gravity, model EGM2008 is illustrated on map with relocated seismicity and tectonic structures (Figure 4.10), where free air gravity values varies from -200mGal to 450mGal in the study area. The very low (negative) gravity indicates deep low density crustal thinning in the NW while the gradual increase (positive)in northeast of study area suggests the crustal thickening of Indian plate in this direction. The map suggested that the Besham Dom and IKSZ are the thick-skinned blind basement faults whereas the MMT is a suture zone that separates the Indian Plate from KLA (Khan et al., 2023).

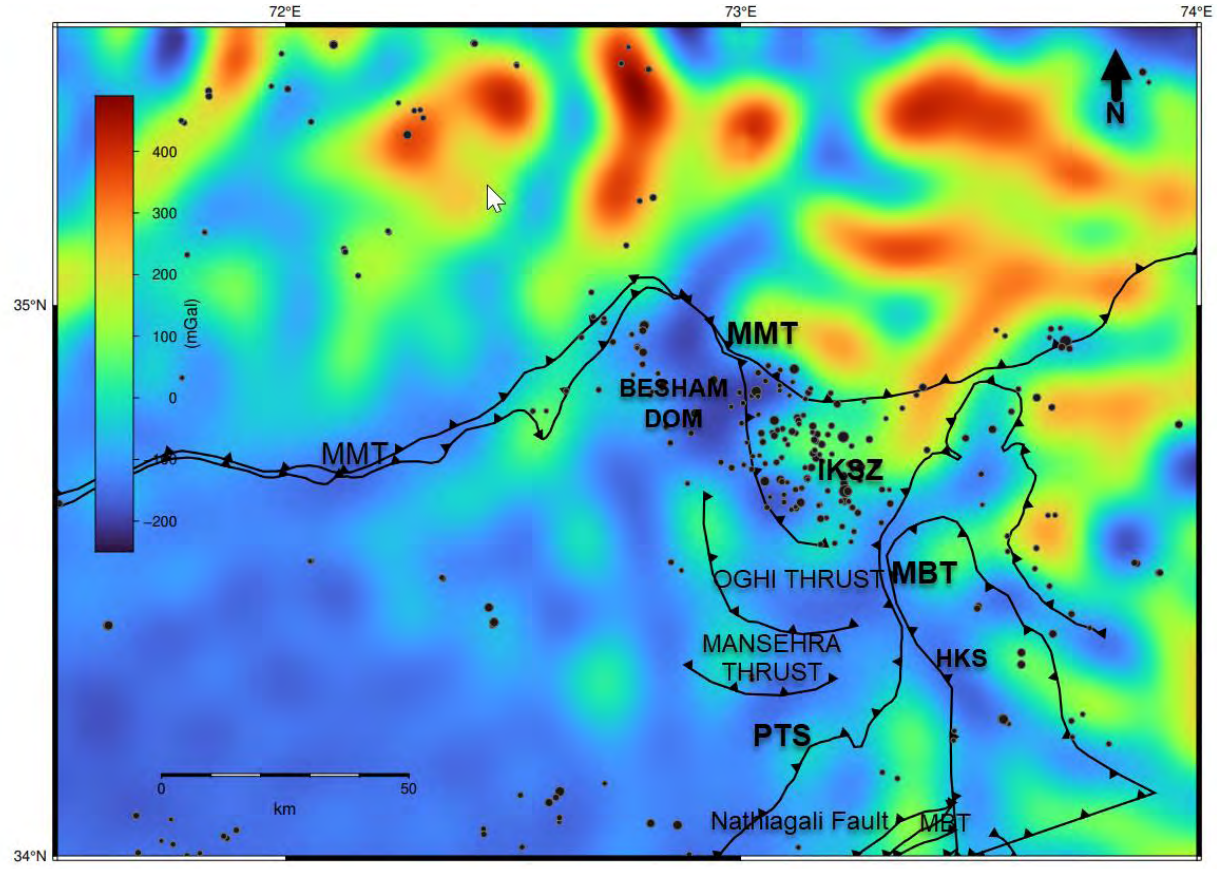

Figure 4.10: The Map Illustrates Free Air gravity (EGM2008) and relocated seismicity distribution with tectonic structures.

3.4 Cross-Sections

Cross-sections are useful tools to analyze tectonic settings, fault properties and seismogenic environment investigations. We selected three cross-sections along and three across the MMT presented in Figures 4.11 to 4.16. The location of each profile is marked (Figure 4.6) and presented y-axis with depth scale 0 to 60 km, gravity scale -250mGal to 450 mGal and x-axis as distance 0 to 75 km (Figure 4.11 to 4.16). We superimposed relocated seismicity within the window width of ±10 km on each. The initial horizontal, vertical and depth direction position were 1174 m, 733 m, and 2707 m respectively while after relocation horizontal, vertical and depth position were 145 m, 98 m, and 89 m. Furthermore, we can also infer the geometry of faults using these profiles.

Profile AA'

In Profile AA′, which is across the MMT (Figure.4.6), the depth of relocated earthquakes is observed from 5-20 km. The result showed that earthquakes mainly occurred between -100 mGal and 80mGal (Figure 4.11). Moreover, the changes in gravity were abrupt and inconsistent while few earthquakes occurred between 21 km and 35 km depth. The low free air gravity and dense seismicity in the IKSZ, suggests a region of active tectonic processes such as stress accumulation, density variation, crustal thinning /thickening or presence of thrust faulting due to Indian and Eurasian plates collision.

The seismicity pattern down to 35 km depth has low dip that depicted by the dip ≤45° NE and orientation NW-SE, which is in general agreement with the focal mechanism no. 4 (Table 4) having dip range from 40° to 56° NE and strikes in NE-SW.

Gravity showed sharp changes near high seismicity and associated with low gravity. NE trend of seismicity at the edge of profile was matched with NE trend of MMT justify the earthquake relocation method affectivity to identify seismogenic structure's orientation. FMS presented in figure demonstrate strike as NE strike oriented and low dip angle which is consistent with relocated seismicity orientation.

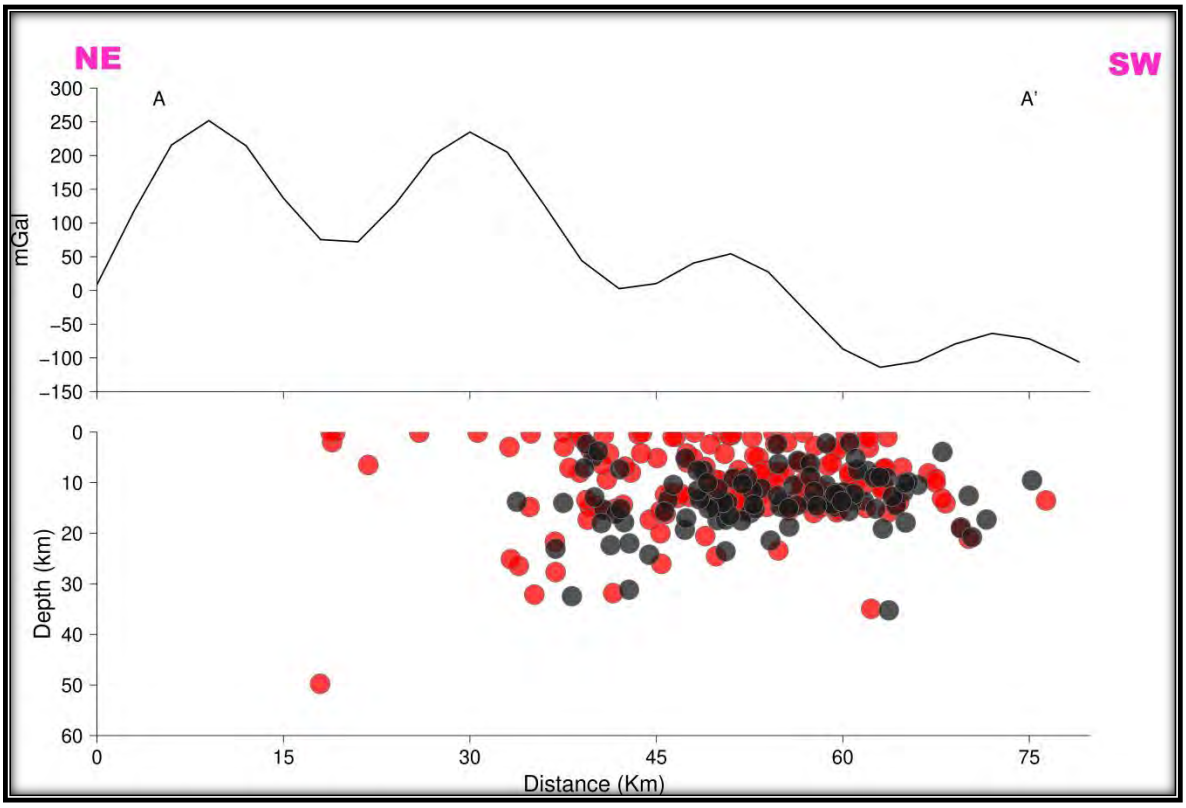

Figure 4.11: The top panel illustrates the gravity value along the profile AA'. The gravity value is obtained from EGM2008 model. The bottom panel illustrates the initial locations of earthquakes (red circles and relocated earthquakes (black circles) along the profile AA.'

Profile BB'

In profile BB' (Figure 4.12) depth of relocated earthquakes observed more clustered at depth 5-20 km and distance between 30 to 60km. Overall, gravity is observed very low over seismicity which have range -140 mGal to -20 mGal. Within the given range, gravity showed sharp changes near dense seismicity but changes of gravity values at edges cannot be associated

with seismicity due to unavailability of data. The possible interpretation could be that region low gravity over dense seismicity indicates active tectonic processes such as presence of seismogenic thrust fault and low density caused by crustal thinning or transition zone between tectonic domains.

NE trend and low dip angle about 40^0 of seismicity at the edge of profile was matched with FMS n0. 7 dip 31^0 to 60^0 NE-SW orientations which confirmed geometry of thrust faults present in the vicinity of MMT that justify the earthquake relocation method affectivity to identify seismogenic structure's orientation.

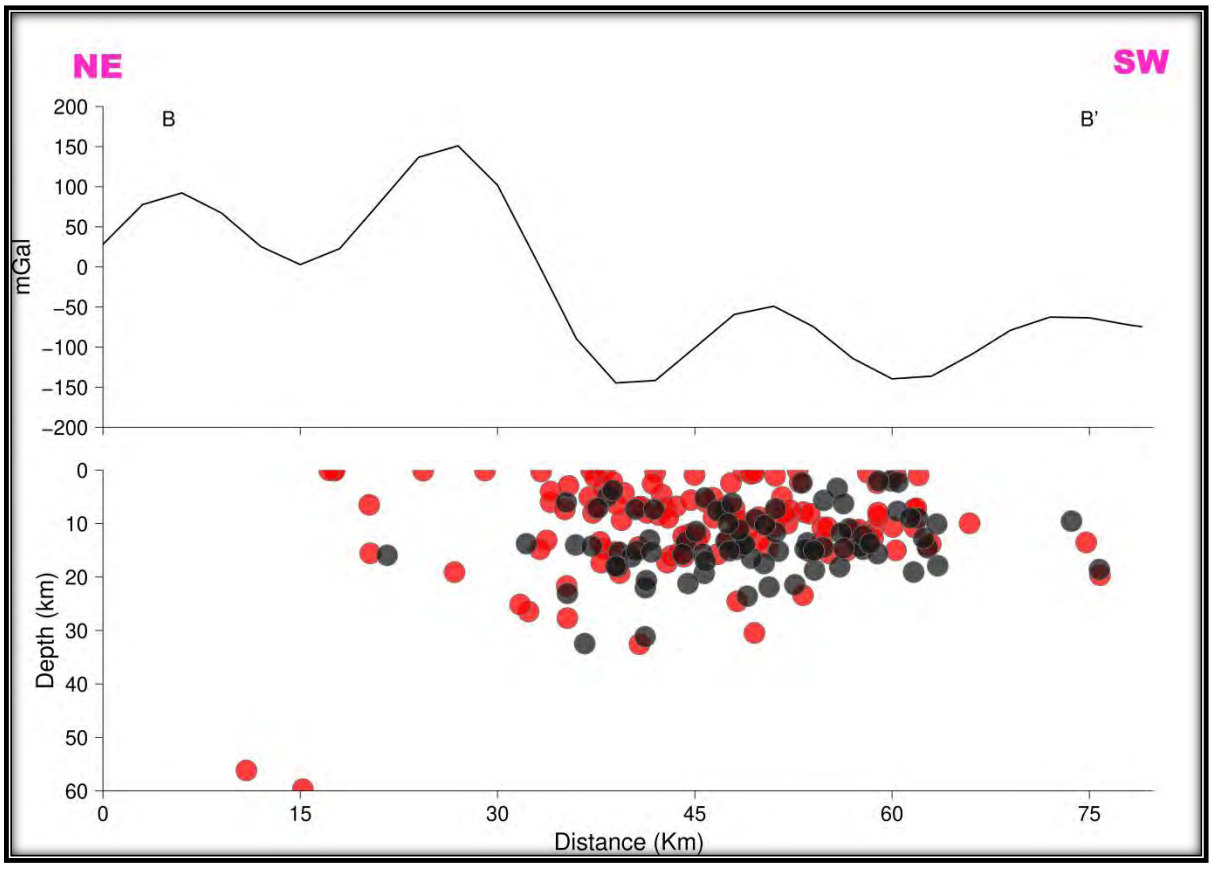

Figure 4.12: The top panel illustrates the gravity value along the profile BB'. The gravity value is obtained from EGM2008 model. The bottom panel illustrates the initial locations of earthquakes (red circles and relocated earthquakes (black circles) along the profile BB'.

Profile CC'

In profile CC'(Figure 4.13) depth of clustered relocated earthquakes was observed at 3 to 30 km while few deep earthquakes were observed up to 50 km as well. The dense seismicity distribution observed from distance 0 to 35 km while there was sparse distribution of seismicity from distance 35 to 75 km.

Gravity showed overall sharp changes throughout the profile. Decreasing trend of low gravity range -200 mGal to -100 mGal on graph was observed from distance 0 to 30 km where dense seismicity distribution observed and increasing trend from -100 mGal to 200 mGal observed where seismicity was sparsely distributed. The steep gradient of free air gravity can possibly suggest the highly deformed zone due Indian plate under thrusting blow IKSZ.

NE trend and dip $\geq 35^0$ of seismicity at the edges of profile was matched with NE trend of MMT which demonstrates the earthquake relocation method affectivity to identify seismogenic structure's orientation.

Moreover, FMS no. 4 presented (Table 4) gave information of NW-SE strike as orientation and dip range 40^0 to 56^0 which was nearly consistent with relocated seismicity orientation.

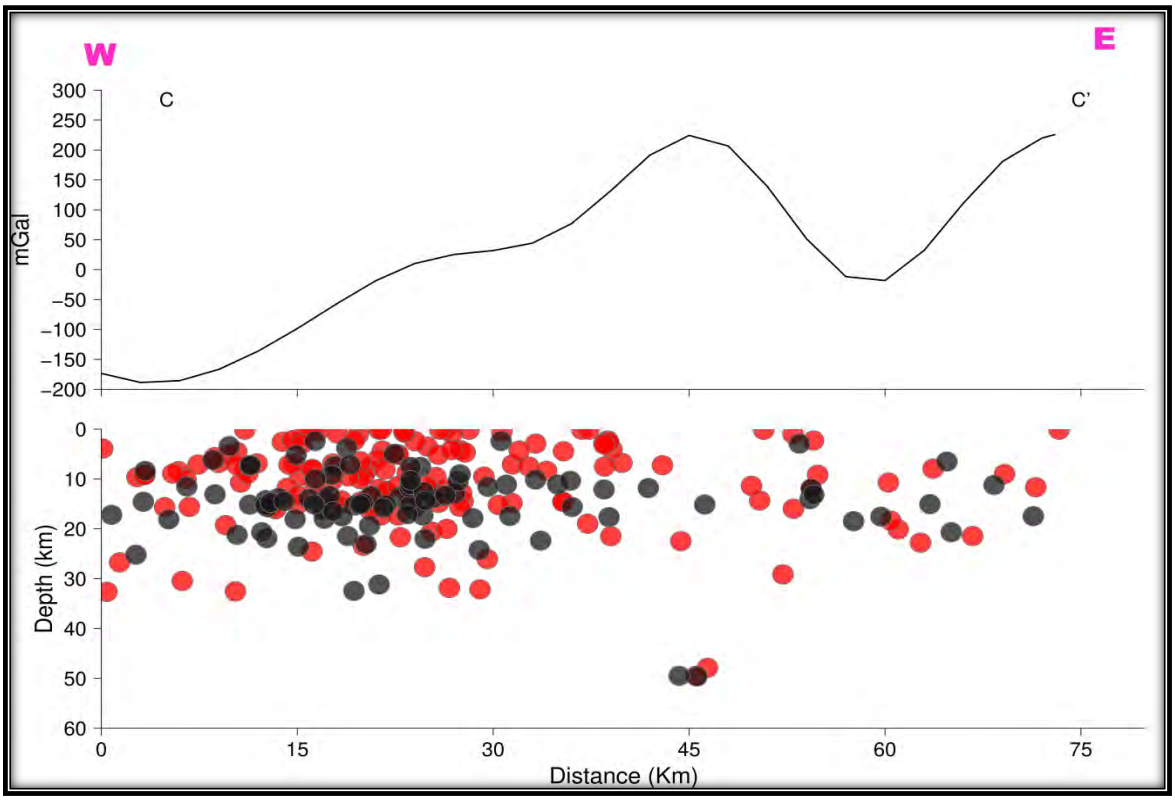

Figure 4.13: The top panel illustrates the gravity value along the profile CC''. The gravity value is obtained from EGM2008 model. The bottom panel illustrates the initial locations of earthquakes (red circles and relocated earthquakes (black circles) along the profile CC'.

Profile DD'

In profile DD'(Figure 4.14) depth of clustered relocated earthquakes was observed at 5 to 17 km while few earthquakes were observed up to 35 km as well. The dense seismicity distribution observed from distance 45 to 70 km where gravity showed abrupt changes from -80 mGal to 100 mGal. Positive gravity indicates crustal thickening or presence high-density ultramafic rocks in the region while negative gravity suggests deeper low angle basement.

NE trend and dip $\geq 40^0$of seismicity pattern was observed consistent with NE trend MMT which demonstrates the earthquake relocation method affectivity to identify seismogenic

structure's orientation. FMS no. 3 presented (Table 4) gave information of NE as orientation and dip range 43^0 to 48^0 which confirmed relocated seismicity orientation with the possible thrust seismogenic structure.

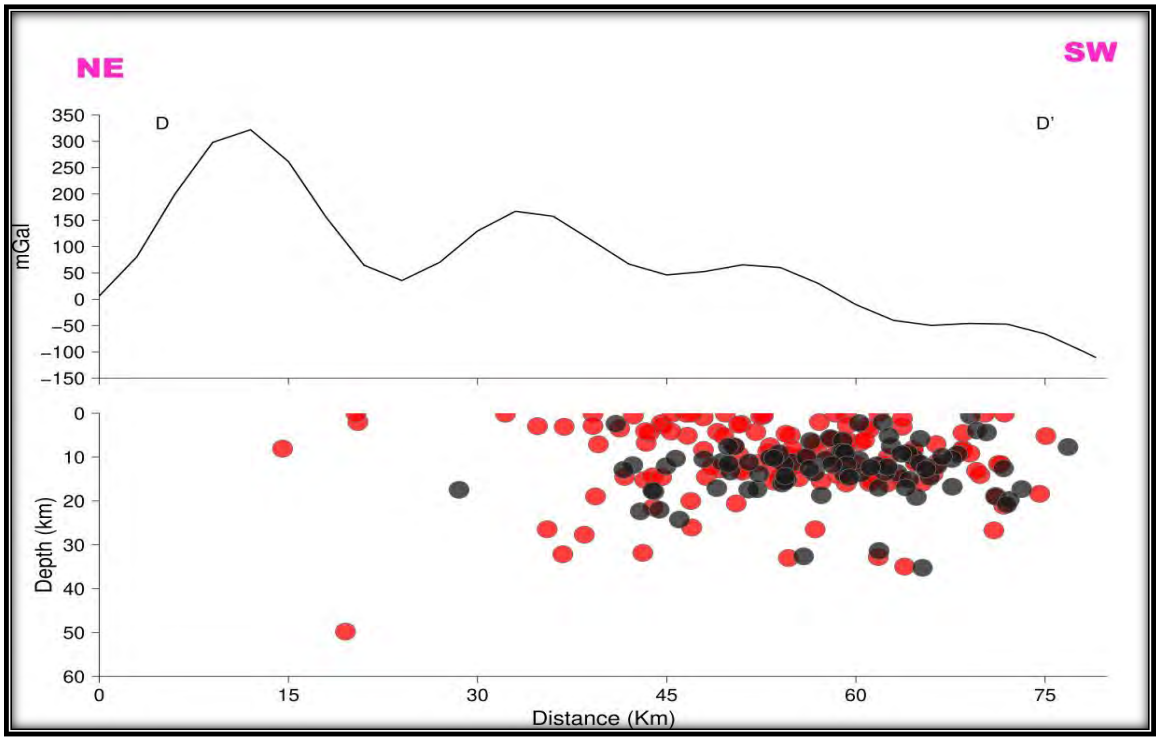

Figure 4.14: The top panel illustrates the gravity value along the profile DD'. The gravity value is obtained from EGM2008 model. The bottom panel illustrates the initial locations of (red circles and relocated earthquakes (black circles) along the profile DD'.

Profile EE'

In profile EE' (Figure 4.15) depth of clustered relocated earthquakes was observed at 3 to 25 km while few earthquakes were observed up to 45 km as well. The dense seismicity distribution observed from distance 10 to 40 km and sparse distribution observed between 50 and 70 km.

Gravity showed sharp gradient have values range -100 mGal to 80 mGal where dense seismicity was observed. The negative gravity values from 0 to 30 km distance and sharp

change in the trend of the free air anomaly is can be attributed to the Besham basement rocks which are also exposed on the surface. The positive values show a very steep gravity gradient in the northeast direction and suggested the presence of thick-skinned blind basement IKSZ.

The orientation of seismicity pattern is likely to be in NE and the observed angle ranged from 35^0 to 45^0 which were conformable with NE trend of MMT. It showed that the HypoDD method is affectively identifying seismogenic structure's orientation. Moreover, FMS no. 3 and 6 presented (Table 4) information of NE-SW strike as orientation and dip range 39^0 to 53^0 which was somehow consistent with the relocated seismicity orientation with the possible oblique slip seismogenic structure.

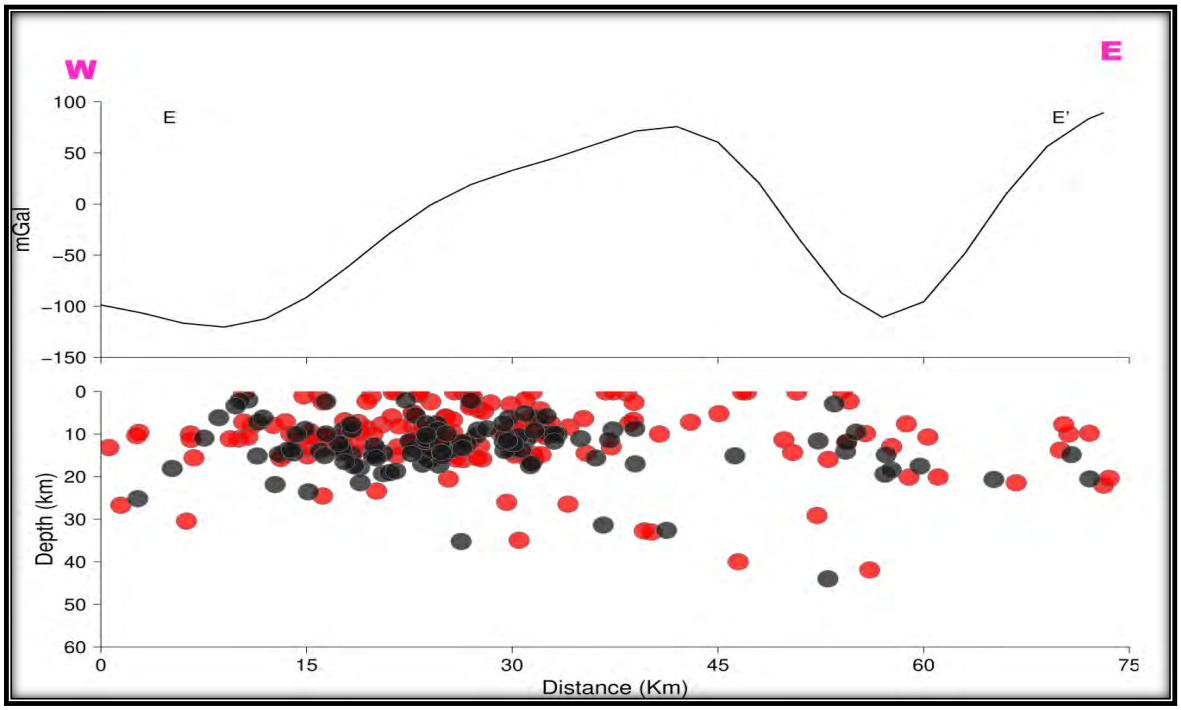

Figure 4.10: The top panel illustrates the gravity value along the profile EE'. The gravity value is obtained from EGM2008 model. The bottom panel illustrates the initial locations of (red circles) and relocated earthquakes (black circles) along the profile EE'.

Profile FF'

In profile FF' (Figure 4.16) seismicity distribution is not clustered instead dispersed from shallow depth 5 to 40km with some deeper earthquakes. Gravity gradient -150 mGal to 80 mGal to some extents was associable with seismicity distribution. For example, low negative free air gravity interpreted the presence of MMT and possible presence of low density rocks. As seismicity is dispersed and unavailability of high-quality FMS, inference of seismogenic structure orientation is difficult.

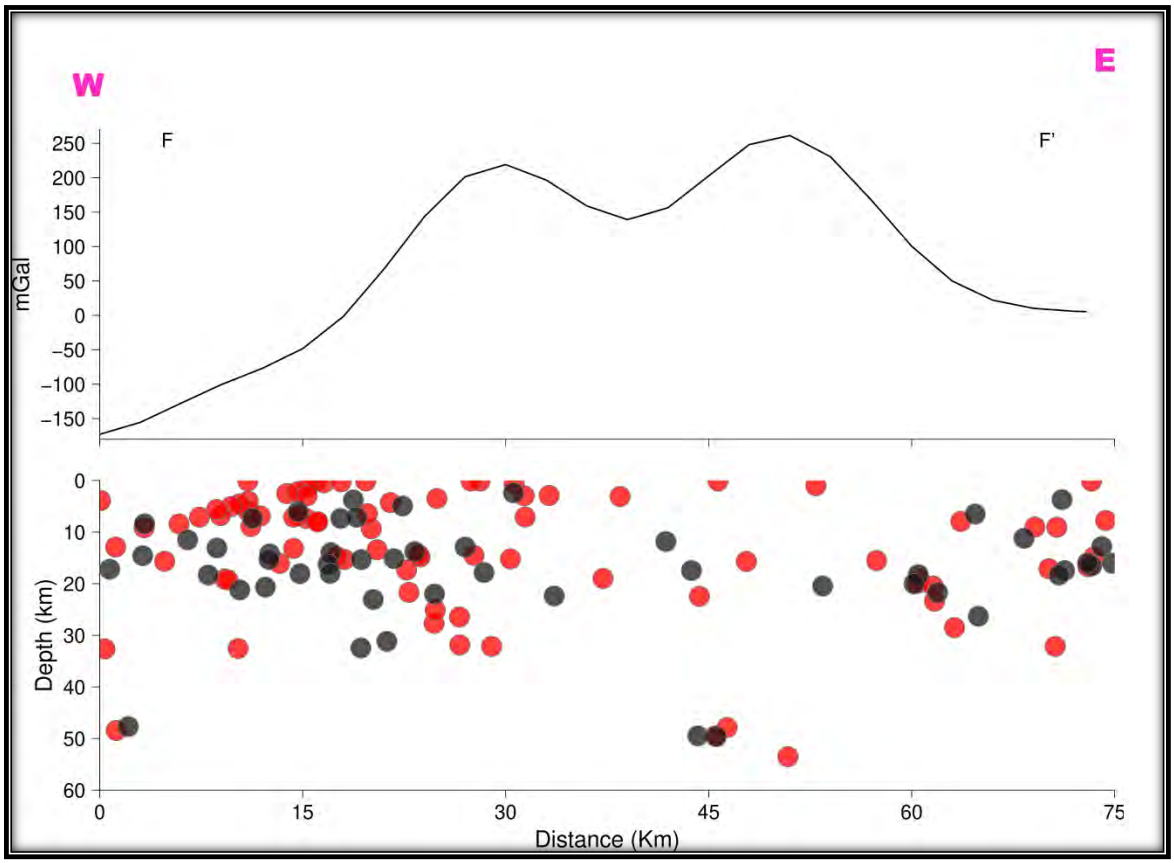

Figure 4.16: The top panel illustrates the gravity value along the profile FF'. The gravity value is obtained from EGM2008 model. The bottom panel illustrates the initial locations of (red circles and relocated earthquakes (black circles) along the profile FF'.

It is possible to evaluate the geometry of seismogenic faults and their stress fields by studying the distribution of relocated seismic earthquakes. Figure (4.6) shows the map view and

6 cross-sections of seismic earthquakes with M_L>2.0 distribution along and perpendicular to the MMT, MBT and the focal mechanisms of earthquakes with $M_L \geq 5.0$. The uncertainties of the crustal model, especially the lateral heterogeneities of the upper crust, do not lead to significant changes in the interpretation of seismogenic structures in IKSZ.

Earthquakes mainly occurred on different faults that were low angle each other, and the focal depths are mainly between 3 km and 20 km (Figure. 4.4, 4.6). In the study, there was observed a dense earthquake cluster at depths between 3 km and 20 km as shown in DD′ and EE' profiles. In cross-section EE′, we observe diffuse seismicity, not defining a clear fault plane. In cross-sections FF′, a nearly low angle alignment of earthquakes is visible down to the depth of 20, then dipping eastward. In other cross-sections a nearly low angle seismicity is clearly visible almost along the whole thrust fault.

One of the purposes of this study was to examine the seismicity of eastern side of MMT regarding particular geological structures or geophysical anomalies. For this purpose, there was constructed cross-section of free air gravity with relocated seismicity. There were observed low free air gravity anomalies and sharp gradient which indicate the presence of faults, crustal thinning /thickening and low density deformed zones (Subrahmanyam et al., 1995).

The observed distribution of seismicity and found that most of the earthquakes recorded were located in the valley and ridge province where gravity has sharp gradient in profiles AA', BB', CC', DD', EE' and FF' (between distance 0-30 and 60-75 km). This observation differs from the historical seismicity pattern, which was dispersed into some (western) part of MMT as observed in profiles.

Conclusion

To conclude, the current work used the double difference relative earthquake relocation or HypoDD method to minimize error in hypocentral locations and to identify seismogenic structure in the eastern side of the Main Mantle Thrust in the NW Himalayas, Pakistan. From 2010 to 2021, total 15561 earthquakes were recorded across 25 stations and were obtained from the Micro Seismic Monitoring System (MSMS) WAPDA. To localize the earthquakes, the current study utilized 130043 P phases and 56107 S phases. 6426 earthquakes are relocated by the HypoDD algorithm and the region's seismogenic structure's determined using findings, relocated seismicity, the Free Air Gravity Model (EGM2008), and Focal Mechanism Solutions (FMS).

According to the findings, the HypoDD approach decreased the residual travel time, which was 66 ms as compare to the original 154 ms. after earthquake relocations; it has been shown that most earthquake clusters observed at a depth of 3 to 30 km on average, with a few occurring at a depth of 50 km. A low dip angle and a NE trend in the seismicity distribution pattern found in the agreement of focal mechanism solutions explanations that indicated the presence of thrust faults with a minor component of strike slip close to the MMT. Moreover, the current research especially focused on the Indus Kohistan Seismic Zone (IKSZ), which is thought to be the most tectonically active region, and estimated northeast-trending faults there. A significant correlation between a steep gradient in free air gravity and dense seismicity was also found. The study's findings are thus examined in the context of earlier work.

Limitations, Suggestions and Implication of the Study

The present study has two limitations. One is the azimuthal coverage and spars distribution of stations and the second limitation is the unavailability of cross-correlation data. Future researches needs to use cross correlational data in order to increase the reliability/accuracy of the results as well as to generalize the findings across different regions.

The findings of present study are helpful to understand the seismicity in the active seismic zones in NW Himalayas. The findings like improved hypocentral locations, fault orientation and seismogenic structures are important factors in the comprehension of seismicity. In addition, the relocated hypocenters can aid in improving velocity model and developing effective feasibility studies for tomography as well as hazard analysis in the study region. Moreover, areas with steep topographic relief and free air gravity anomalies over seismic gaps should be taken into consideration as possibly hazardous regions where future large earthquakes may occur.

References

Aki, K., and P. G. Richards (1980). Quantitative Seismology, *W. H. Freeman, New York.2,* Derived from https://cir.nii.ac.jp/crid/1574231873863699968

Babar, A. (2014). Preliminary Study of Reservoir Triggered Seismicity in the Vicinity of Tarbela Dam. *Pakistan Journal of Meteorology*, *11*(21).212-231

Bassin, C. (2000). The current limits of resolution for surface wave tomography in North America. *Eos Trans. AGU*, *81*(48), 897-908

Chave, A. D., D. J. Thomson, and M. E. Ander (1987). On the robust estimation of power spectra, coherences, and transfer functions, *J. Geophys. Res. 92*(1), 633–648

DOI: 10.1029/JB092iB01p00633

Crustal and uppermost mantle velocity structure along a profile across the Pamir and southern Tien Shan as derived from project TIPAGE wide-angle seismic data. *Geophys. J. Int*. 188, 385–407. https://doi.org/10.1111/j.1365-246X.2011.05278.x

Pegler, G., & Das, S. (1998). An enhanced image of the Pamir–Hindu Kush seismic zone from relocated earthquake hypocentres. *Geophysical Journal International*, *134*(2), 573-595. DOI:10.1046/J.1365-246X.1998.00582.X

Dodge, D. (1996), Microearthquake studies using cross-correlation derived hypocenters, Ph.D. thesis, *Stanford University*, 146

Douglas, A. (1967). Joint epicentre determination. *Nature, 215*(5096), 47-48. DOI:10.1038/215047A0

Engen, Ø., Eldholm, O., & Bungum, H. (2003). The Arctic plate boundary. *Journal of Geophysical Research: Solid Earth, 108*(2), 1–17. DOI:10.13140/RG.2.1.3853.1601

Focal Mechanisms or "Beachballs". United States Geological Survey (USGS). Derived from https://www.usgs.gov/programs/earthquake-hazards/focal-mechanisms-or-beachballs

Frechet, J. (1985). *Sismogenese et doublets sismiques* (Doctoral dissertation, Universite Scientifique et Medicale de Grenoble).

Frémont, M. J., & Malone, S. D. (1987). High precision relative locations of earthquakes at Mount St. Helens, Washington. *Journal of Geophysical Research: Solid Earth, 92*(10), 10223-10236. DOI: 10.1029/JB092iB10p10223

Geiger, L. (1910). Herdbestimmung bei Erdbeben aus den Ankunftszeiten. Nachrichten von der Königlichen Gesellschaft der Wissenschaften zu Göttingen, Mathematisch-Physikalische Klasse, 331–349. 1912 transliterated in English by FWL Peebles & AH Corey: Probability method for the determination of earthquake epicenters from the arrival time only. *Bulletin St. Louis University, 8*(1), 60-71.

Got, J.-L., J. Fréchet & F.W. Klein (1994), Deep fault plane geometry inferred from multiplet relative relocation beneath the south flank of Kilauea, *J. Geophys. R. 99*(15), 15375-15386.

Hameed, F., Khan, M. R., & Dentith, M. (2023). Crustal study based on integrated geophysical techniques in the Northwestern Himalayas, Pakistan. Geological Journal. Special issue and volume 2023 to be published, 1-27. DOI: https://doi.org/10.1002/gj.4672

Iqbal, T., Ali, Z. A. H. I. D., Mahmood, T., Qaisar, M., & AHMAD, N. (2008). Seismic Microzoning Of Upper Hazara Region, Based On Impact Analysis Of Recent Earthquakes. *Geol. Bull. Punjab Univ*, 43(2008), 109-119.

Johnson, M., & Vincent, C. (2002). Development and testing of a 3D velocity model for improved event location: A case study for the India-Pakistan region. *Bulletin of the Seismological Society of America, 92*(8), 2893-2910. DOI:10.1785/0120010111

Johnson, M.R.W., (2002). Shortening budgets and the role of continental subduction during the India-Asia collision. *Earth-Science Rev. 59*(1):101-123.

DOI: 10.1016/S0012-8252(02)00071-5

Kennett, B. L. N., & Engdahl, E. R. (1991). Traveltimes for global earthquake location and phase identification. *Geophysical Journal International*, *105*(2), 429-465.. DOI:10.1111/j.1365-246X.1991.tb06724.x

Khwaja, A. A., & Qureshi, S. N., Mona Lisa (2005). Structural interpretation on the basis of focal mechanism studies in the area of Kohat Plateau, Bannu Basin and western extension of Salt Range. *Pakistan Journal of Hydrocarbon Research*, *15*, 43-51

Kim, K. H., Chiu, J. M., Pujol, J., & Chen, K. C. (2005). Earthquake relocations, fault zone geometry and constraints on lateral velocity variations using the joint hypocenter determination method in the Taiwan area. *Earth, planets and space, 57*(9), 809-823. http://doi.org/10.1186/BF03351860.

Klein, F.W. (1989), User's Guide to HYPOINVERSE, a program for VAX computers to solve for earthquake locations and magnitude, *U.S.G.S.* 89-314. DOI: https://doi.org/10.3133/ofr89314

Koulakov, I., Sobolev, S. V., (2006). A tomographic image of Indian lithosphere break-off beneath the Pamir-Hindukush region. *Geophys. J. Int. 164*, 425–440. https://doi.org/10.1111/j.1365- 246X.2005.02841.x

Li, A., Mashele, B., (2009). Crustal Structure in the Pakistan Himalaya from teleseismic receiver functions. *Geochemistry, Geophys and Geosystems 10*(12), 1–11.

https://doi.org/10.1029/2009GC002700

Li, C., van der Hilst, R.D., Meltzer, A.S., Engdahl, E.R., (2008). Subduction of the Indian lithosphere beneath the Tibetan Plateau and Burma. Earth Planet. *Sci. Lett. 274*, 157–168. https://doi.org/10.1016/j.epsl.2008.07.016

Mahdi, S. K., (1988). Reservoir A Question of Induced Seismicity. Proceedings: Second International Conference on Case Histories in Geotechnical Engineering, *Scholars' Mine*. 1663 – 1667.

Maneno, R., Sentosa, B. J., & Rachman, G. (2019). Relocation Of Earthquake Hypocenter In The Flores Region Using Hypo71. *IPTEK The Journal of Engineering, 5*(2), 33-37. DOI: http://dx.doi.org/10.12962/j23378557.v5i2.a5024

Martin, A. J. (2017). A review of Himalayan stratigraphy, magmatism, and structure. *Gondwana Research, 49*(2017), 42–80. DOI: https://doi.org/10.1016/j.gr.2017.04.031

Mechie, J., Yuan, X., Schurr, B., Schneider, F., Sippl, C., Ratschbacher, L., Minaev, V., Gadoev, M., Oimahmadov, I., Abdybachaev, U., Moldobekov, B., Orunbaev, S., Negmatullaev, S., (2012). Crustal and uppermost mantle velocity structure along a profile across the Pamir and southern Tien Shan as derived from project TIPAGE wide-angle seismic data. *Geophysical Journal, 188*(2), 385-407. DOI:S 10.1111/j.1365-246X.2011.05278.x

Menke, W. (1999). Using waveform similarity to constrain earthquake locations, *Bull. Seism. Soc. Am.* 89, 1143–1146.

Michael, A. J. (1988). Effects of three-dimensional velocity structure on the seismicity of the 1984 Morgan Hill, California, aftershock sequence, *Bull. Seism. Soc. Am*. 78, 1199–1221.

Ni, J.F., Ibenbrahim, A., Roecker, S.W., (1991). Three-dimensional velocity structure and hypocenters of earthquakes beneath the Hazara Arc, Pakistan: Geometry of the underthrusting Indian Plate. *Journal of Geophysical Research: Solid Earth. 96*(12), 19865-19877 https://doi.org/10.1029/91JB02103

Paige, C.C. and M.A. Saunders (1982), LSQR: Sparse linear equations and least squares problems, *ACM Transactions on Mathematical Software 8*(2), 195-209. DOI: 10.1145/355993.356000

Pavlis, N. K., Holmes, S. A., Kenyon, S. C., & Factor, J. K. (2008). An Earth Gravitational Model to Degree 2160: EGM2008; presented at the 2008 General Assembly of the European Geosciences Union, Vienna, Austria, April 13–18. *Monograph of precise levelling networks in Poland (in polish)*.

Poupinet, G., Ellsworth, W. L., & Frechet, J. (1984). Monitoring velocity variations in the crust using earthquake doublets: An application to the Calaveras Fault, California. J*ournal of Geophysical Research: Solid Earth, 89*(7), 5719-5731. DOI: https://doi.org/10.1029/JB089iB07p05719

Pujol, J. (2000). Joint event location—the JHD technique and applications to data from local seismic networks. Advances in seismic event location, 18(), 163-204.

DOI: 10.1007/978-94-015-9536-0_7

Replumaz, A., Negredo, A. M., Guillot, S., & Villaseñor, A. (2010). Multiple episodes of continental subduction during India/Asia convergence: Insight from seismic tomography and tectonic reconstruction. Tectonophysics, 1(2),125-134. DOI:https://doi.org/10.1016/j.

Riaz, M. S., Zheng, Y., Xiong, X., Xie, Z., Li, Z., & Song, M. (2017). Refined 3D Seismic-Velocity Structures and Seismogenic Environment of the Ms 6.5 Ludian EarthquakeRefined 3D Seismic-Velocity Structures and Seismogenic Environment of the Ms 6.5 Ludian Earthquake. *Bulletin of the Seismological Society of America, 107*(6), 3023-3036. DOI: https://doi.org/10.1785/0120170072

Richards-Dinger, K.B., & Shearer, P.M. (2000), Earthquake locations in southern California obtained using source-specific station terms, J. Geophys. R. 105(5), 10939-10960.

DOI: https://doi.org/10.1029/2000JB900014

Sana, H., & Nath, S.K., (2016). In and Around the Hazara-Kashmir Syntaxis : a Seismotectonic and Seismic Hazard perspective. *J. Ind. Geophys. Union 20*(5), 496–505.

Schaff, D. P., & Waldhauser, F. (2005). Waveform cross-correlation-based differential travel-time measurements at the Northern California Seismic Network. Bulletin of the *Seismological Society of America, 95(*6), 2446-2461.

DOI: https://doi.org/10.1785/0120040221

Schweitzer, J., Storchak, D. A., & Borman, P. (2019). Seismic phase nomenclature: The IASPEI standard. *Encyclopedia of Solid Earth Geophysics,* 1-13. DOI: https://doi.org/10.1007/978-3-030-10475-7_11-1

Searle, M., Khan, M.A., Fraser, J., Gough, S. and Jan, M. Q. (1999) The tectonic evolution of the Kohistan Karakoram collision belt along the Karakoram Highway transect, north Pakistan. *Tectonics, 18*(6), 929- 949.

Seeber, L., Quittmeyer, R., Armbruster, J., (1980). Seismotectonics of Pakistan: a review of results from network data and implications for the central Himalayas. *Geol Bull Univ Peshawar, 13*(1), 151–168.

Shehzad, Z., & Yokoi, T. (2013). 1-D Velocity Model For Wapda Tarbela Microseismic Network In Tarbela And Northern Areas, Pakistan. *Bulletin of the International Institute of Seismology and Earthquake Engineering, 47(*1), 43-48.

Shah, S. F. H., Ningsheng, C., Khaliq, A. H., Alam, M., Ahmad, H., & Rahman, M. (2022). Probabilistic Seismic Hazard Analysis of Hazara Kashmir Syntaxes and its Surrounding. *Journal of the Geological Society of India, 98*(9), 1308-1319. DOI:10.1007/s12594-022-2167-y

Spence, W. (1980). Relative epicenter determination using P-wave arrival-time differences. *Bulletin of the Seismological Society of America, 70*(1), 171-183.

Stein, S., & Okal, E. A. (2005). Speed and size of the Sumatra earthquake. *Nature, 43*(33), 581-582. DOI: https://doi.org/10.1038/434581a

Subrahmanyam, V., Rao, D. G., Ramana, M. V., Krishna, K. S., Murty, G. P. S., & Gangadhara, M. (1995). Structure and tectonics of the southwestern continental margin of India. Tectonophysics, 249(3-4), 267-282. DOI: 10.1016/0040-1951(95)00020-N

Thakura, V. C., Jayangondaperumal, R. & Malik, M. A. (2010). Redefining Medlicott–Wadia's main boundary fault from Jhelum to Yamuna: An active fault strand of the main boundary thrust in northwest Himalaya. *Tectonophysics, 489*(1), 29–42.

DOI: 10.1016/j.tecto.2010.03.014

Tiwari, V. M., Rajasekhar, R. P., & Mishra, D. C. (2009). Gravity anomaly, lithospheric structure and seismicity of Western Himalayan Syntaxis. *Journal of seismology, 13*(3), 363-370. DOI: 10.1007/s10950-008-9102-6

Turquet, A. L., Bodin, T., Arroucau, P., Sylvander, M., & Manchuel, K. (2019). Quantifying location uncertainties in seismicity catalogues: application to the Pyrenees. *Journal of Seismology*, *23*(2), 1097-1113. DOI: 10.1007/s10950-019-09857-8

Van Der Voo, R., Spakman, W., Bijwaard, H., (1999). Tethyan subducted slabs under India. Earth Planet. *Sci. Lett. 171*(1), 7–20. DOI: https://doi.org/10.1016/S0012-821X(99)00131-4

Verma, R. K., & Prasad, K. A. V. L. (1987). Analysis of gravity fields in the northwestern Himalayas and Kohistan region using deep seismic sounding data. Geophysical Journal International, 91(3), 869-889. DOI: https://doi.org/10.1111/j.1365-246X.1987.tb01672.x

W. Spence, (1980) "Relative epicenter determination using P-wave arrival-time differences," *Bull. Seismol. Soc. Am. 70* (1). 171–183. DOI: 10.1785/BSSA0700010171.

Waldhauser, F. (2001). HYPODD--A program to compute double-difference hypocenter locations, U.S. Geologic Survey Open-File Report. DOI: 10.7916/D8SN072H. Derived from. https://pubs.er.usgs.gov/publication/ofr01113

Waldhauser, F. and W.L. Ellsworth (2000). A double-difference earthquake location algorithm: Method and application to the Hayward fault. *Bulletin of the Seismological Society of America 90*(6), 1353-1368. DOI: https://doi.org/10.1785/0120000006

Watt, J., Ponce, D., Parsons, T., & Hart, P. (2016). Missing link between the Hayward and Rodgers Creek faults. *Science advances, 2*(10), e1601441. DOI: 10.1126/sciadv.1601441

Wheeler, R. L. (1995). Earthquakes and the cratonward limit of Iapetan faulting in eastern North America. *Geology, 23*(2), 105-108. DOI: https://doi.org/10.1130/0091-7613(1995)023<0105

Wolfe, C.J. (2002). On the mathematics of using difference operators to relocate earthquakes. *Bulletin of the Seismological Society of America 92*(8), 2879-2892. DOI: https://doi.org/10.1785/0120010189

Wu, X., Huang, S., Xiao, Z., & Wang, Y. (2022). Building Precise Local Submarine Earthquake Catalogs via a Deep-Learning-Empowered Workflow and its Application to the Challenger Deep. *Frontiers in Earth Science, 10*(1), 34. DOI:10.3389/feart.2022.817551

Yeats, R. S., T. Nakata, A. Farah, M. Fort, M. A. Mirza, M. R. Pandey, and R. S. Stein, 1992: The Himalayan frontal fault system, Ann. *Tecton. 6*(1), 85-98.

Yin, A., 2006. Cenozoic tectonic evolution of the Himalayan orogen as constrained by along strike variation of structural geometry, exhumation history and foreland sedimentation. *Earth Sci. Rev. 76*(1, 2), 1–131. DOI: https://doi.org/10.1016/j.earscirev.2005.05.004

Yoshida, M., Zaman, H., Ahmad, M.N., (1996). Paleoposition of Kohistan arc and surrounding terranes since Cretaceous time: the paleomagnetic constraints, in: Proceedings of Geoscience Colloquium, Geoscience Laboratory, *Geological Survey of Pakistan. 15*(83), 83–101.

Zaman, H., Torii, M. (1999). Palaeomagnetic study of Cretaceous red beds from the eastern Hindukush ranges, northern Pakistan: palaeoreconstruction of the Kohistan–Karakoram composite unit before the India–Asia collision. *Geophysical Journal International*, *136*(3), 719-738.DOI: https://doi.org/10.1046/j.1365-246x.1999.00757.x

Zhou, Z., Lei, J., (2016). Pn anisotropic tomography and mantle dynamics beneath China. Phys. Earth Planet. *Inter*. 257, 193–204. https://doi.org/10.1016/j.pepi.2016.06.005